

OPTICAL PROPERTIES OF CAD-CAM LITHIUM DISILICATE  
GLASS-CERAMIC IN DIFFERENT FIRING  
TEMPERATURES AND THICKNESSES

By

Nasser Alqahtani

Submitted to the Graduate Faculty of the School of Dentistry in partial fulfillment of the degree of Master of Sciences in Dentistry, Indiana University School of Dentistry, 2016

Thesis accepted by the faculty of the Department of Prosthodontics, Indiana University, in partial fulfillment of the requirements for the degree of Master of Sciences in Dentistry.

Dean Morton

Kamolphob Phasuk

Tien-Min Gabriel Chu  
Chair of the Committee

John A. Levon  
Program Director

Date \_\_\_\_\_

DEDICATION

This thesis is dedicated to my parents for their support, love, and patience, which were my inspiration to success.

## ACKNOWLEDGMENTS

First, I want to thank God for giving me the health to continue my study and reach this level of education.

I would like to convey my deepest gratitude to the Ministry of Higher Education and King Khalid University College of Dentistry in Saudi Arabia for their scholarship and financial support that helped me continue my graduate education.

I would like to express the deepest appreciation to Dr. Tien-Min Gabriel Chu for his great guidance and contributions in this thesis, and Dr. Kamolphob Phasuk for his guidance, help and support throughout the writing of this thesis. I also would like to thank my research committee members, Dr. John Levon and Dr. Dean Morton for their guidance and suggestion and help throughout my research project.

Special thanks to our dental assistants in the graduate prosthodontics clinic for their help and support in the clinics, Ms. Cindy Corbin for her support and kindness, and Ms. Qing Tang and Mr. George Eckert for their works on the statistical analysis for the research. Also, a special thanks to Dr. Ding Li for her help and guidance during samples preparation and data analysis.

Finally, I would like to thank my family, my friends, and all Indiana University staff members for their patience, help, and support throughout my study.

TABLE OF CONTENTS

Introduction.....	1
Review of Literature .....	6
Materials and Methods.....	33
Results and Discussion .....	38
Figures and Tables .....	46
Summary and Conclusions .....	119
References.....	121
Abstract.....	127
Curriculum vitae	



LIST OF FIGURES AND TABLES

FIGURE 1.	Diamond saw (Isomet 1000, Buehler, Lake Forest, IL).....	47
FIGURE 2.	Ivoclar Vivadent ceramic furnace (Programat® CS).....	48
FIGURE 3.	Samples were ready for firing .....	49
FIGURE 4.	Samples after firing in three temperatures .....	50
FIGURE 5.	Diagram of the study design.....	51
FIGURE 6.	Spectrophotometer (CM-2600D) .....	52
FIGURE 7.	Samples with different thicknesses on a white and black background	53
FIGURE 8.	Managing Accurate Resin Curing (MARC®), resin calibrator.....	54
FIGURE 9.	A sample placed between the bottom sensor of the resin calibrator and the curing light tip .....	55
FIGURE 10.	The top sensor of the resin calibrator measuring the mean irradiance of the curing unit light .....	56
FIGURE 11.	Mean irradiance of the recommended group for all thicknesses .....	57
FIGURE 12.	A logarithmic plot of the mean irradiance in each thickness for the HT group.....	58
FIGURE 13.	A logarithmic plot of the mean irradiance in each thickness for the LT group.....	59
FIGURE 14.	Effective incident irradiances for the HT and LT groups in different firing temperatures .....	60
FIGURE 15.	Spectral peaks of the HT group in each thickness for the different firing temperatures .....	61

FIGURE 16.	Spectral peaks of the LT group in each thickness for the different firing temperatures .....	62
FIGURE 17.	Mean CIE L* value for HT and LT group in different firing temperatures .....	63
FIGURE 18.	Mean CIE a* value for both HT and LT groups in different firing temperatures .....	64
FIGURE 19.	Mean CIE b* value for both HT and LT group in different firing temperatures .....	65
FIGURE 20.	Translucency parameter measured from SCI in each thickness of the recommended temperature for HT and LT group .....	66
FIGURE 21.	A logarithmic plot of the translucency parameter measured from SCI in each thickness for the HT group.....	67
FIGURE 22.	A logarithmic plot of the translucency parameter measured from SCI in each thickness for the LT group.....	68
FIGURE 23.	Relation of translucency parameter measured from SCI in each thickness of the recommended temperature for the HT and LT group .	69
FIGURE 24.	TP <sub>0</sub> measured SCI for HT and LT group for each firing temperature ..	70
FIGURE 25.	Translucency parameter measured from SCE in each thickness of the recommended temperature for both HT and LT group .....	71
FIGURE 26.	A logarithmic plot of the translucency parameter measured from SCE in each thickness for the HT group .....	72
FIGURE 27.	A logarithmic plot of the translucency parameter measured from SCE in each thickness for the LT group.....	73

FIGURE 28.	Relation of translucency parameter measured from SCE in each thickness of the recommended temperature for HT and LT groups.....	74
FIGURE 29.	$TP_0$ measured from SCE for both HT and LT group for each firing temperature.....	75
FIGURE 30.	Correlation between the translucency parameter and mean irradiance of both HT and LT group for the recommended temperature .....	76
FIGURE 31.	Correlation between translucency parameter and mean irradiance for all groups .....	77
FIGURE 32.	Correlation between the translucency parameter and contrast ratio measured from SCI of both HT and LT group for the recommended temperature.....	78
FIGURE 33.	Correlation between the translucency parameter and contrast ratio measured from SCE of both HT and LT group for the recommended temperature.....	79
FIGURE 34.	Correlation between the transmission percentage and contrast ratio measure from SCI of both HT and LT group for the recommended temperature.....	80
FIGURE 35.	Correlation between the transmission percentage and contrast ratio measure from SCE of HT and LT group for the recommended temperature.....	81
TABLE I.	Phase formation sequences in the lithium disilicate glass-ceramic.....	82
TABLE II.	The heating schedule of the three different firing temperatures .....	83

TABLE III.	The mean, standard deviation, standard error, minimum and maximum for the mean irradiance ( $\text{mW}/\text{cm}^2$ ).....	84
TABLE IV.	ANOVA results for the maximum for the mean irradiance ( $\text{mW}/\text{cm}^2$ )	85
TABLE V.	Statistical analysis on Mean Irradiance for the recommended temperature group.....	86
TABLE VI.	Statistical analysis on Mean Irradiance for the recommended temperature group (continue) .....	87
TABLE VII.	Summery for the coefficients of absorption .....	88
TABLE VIII.	Summery for the effective mean irradiances.....	89
TABLE IX.	Statistical analysis on Coefficient of Absorption .....	90
TABLE X.	The mean, standard deviation, standard error, minimum and maximum for spectral peak (nm) .....	91
TABLE XI.	ANOVA results for the spectral peak.....	92
TABLE XII.	The mean, standard deviation, standard error, minimum and maximum for CIEL* measured from SCI .....	93
TABLE XIII.	ANOVA results for CIEL* measured from SCI .....	94
TABLE XIV.	The mean, standard deviation, standard error, minimum and maximum for CIEa* measured from SCI.....	95
TABLE XV.	ANOVA results for CIEa* measured from SCI.....	96
TABLE XVI.	The mean, standard deviation, standard error, minimum and maximum for CIEb* measured from SCI.....	97
TABLE XVII.	ANOVA results for CIEb* measured from SCI .....	98

TABLE XVIII.	The mean, standard deviation, standard error, minimum and maximum for CIEL* measured from SCE .....	99
TABLE XIX.	ANOVA results for CIEL* measured from SCE .....	100
TABLE XX.	The mean, standard deviation, standard error, minimum and maximum for CIEa* measured from SCE.....	101
TABLE XXI.	ANOVA results for CIEa* measured from SCE.....	102
TABLE XXII.	The mean, standard deviation, standard error, minimum and maximum for CIEb* measured from SCE.....	103
TABLE XXIII.	ANOVA results for CIEb* measured from SCE.....	104
TABLE XXIV.	The mean, standard deviation, standard error, minimum and maximum for Translucency parameters measured from SCI .....	105
TABLE XXV.	ANOVA results for translucency parameter measured from SCI.....	106
TABLE XXVI.	Statistical analysis on SCI of recommended temperature .....	107
TABLE XXVII.	Statistical analysis on SCI of recommended temperature (continue) .	108
TABLE XXVIII.	Summary of the coefficients of translucency parameters measured from SCI.....	109
TABLE XXIX.	Summary of TP <sub>0</sub> measured from SCI.....	110
TABLE XXX.	Statistical analysis on Coefficient of translucency parameters measured from SCI.....	111
TABLE XXXI.	The mean, standard deviation, standard error, minimum and maximum for Translucency parameters measured from SCE.....	112
TABLE XXXII.	ANOVA results on translucency parameters measured from SCE.....	113

TABLE XXXIII. Statistical analysis on Translucency parameters measured from SCE for the recommended group .....	114
TABLE XXXIV. Statistical analysis on Translucency parameters measured from SCE for the recommended group (continue) .....	115
TABLE XXXV. Summary of the coefficient of translucency parameter measured from SCE.....	116
TABLE XXXVI. Summary for $TP_0$ measured from SCE.....	117
TABLE XXXVII. Statistical analysis on Coefficient of translucency parameter measured from SCE .....	118

## INTRODUCTION



Metal ceramic restoration has been available in dentistry for more than three decades.<sup>1, 2</sup> This type of restoration has gained popularity due to its predictable performance and reasonable esthetics.<sup>3</sup> Despite its success, the demand for improved esthetics and the concerns regarding the biocompatibility of the metal have led to the introduction of all-ceramic restorations.<sup>1, 4</sup> In 1965, McLean was first introduced the aluminous porcelain all-ceramic material as first all-ceramic restoration.<sup>2</sup> Since then, the all-ceramic materials have been evolved for better mechanical and esthetic properties.<sup>2</sup> Traditional all-ceramic materials are brittle with low tensile strength and fracture toughness, potentiating cracks when subjected to stress.<sup>5</sup> Thus, the most common clinical complication of all-ceramic crowns is fracture.<sup>6</sup> Several studies have been conducted to improve the material properties of all-ceramic restorations for optimum clinical outcome.<sup>7</sup> Thus, there are multiple interests of researchers to investigate all-ceramic restoration materials in varying prospective. These include; esthetic and optical properties, physical properties, firing temperatures, method of fabrications, and clinical outcome.<sup>7</sup>

The all-ceramic restoration materials can be generally classified by fabricating techniques or material's microstructural phases.<sup>8</sup> In general, all-ceramic restoration materials can be fabricated by four main techniques including powder-liquid condensation, slip casting, heat-pressed, and computer aided design and computer-aided manufacturing (CAD-CAM) milling.<sup>9</sup> According to material microstructural phases, all-ceramic restorations can be classified into predominantly glass-based, glassy-crystalline, crystalline-based systems with glass fillers and polycrystalline.<sup>10</sup> One of the most

commonly used all-ceramic materials is glassy-crystalline lithium disilicate (LD) material, which was first introduced to dentistry by Ivoclar Vivadent in 1998. This all-ceramic material was called Empress® 2. With the emerging of digital dentistry in computer aided design and especially computer aided manufacturing milling fabrication technique, a multicomponent glass-ceramic blocks such as IPS e.max® CAD LD glass-ceramics were utilized for the benefits of milling, increase cutting efficiency, and maximize the life of the milling tools.<sup>11, 12</sup> IPS e.max® CAD is available in different translucency levels (e.g. low and high translucency). Recently, this material has been used extensively in dental offices due to the ease of use and the high esthetic outcome. However, there is a lack of information in the literature regarding the optical properties of CAD-CAM LD glass-ceramic materials. In this study, we investigated the optical properties of this material as translucency parameter, contrast ratio, light transmission, and color change.

## OBJECTIVES

- 1) To investigate the optical properties as translucency parameters, contrast ratio, light transmissions and color changes between high-translucent and low-translucent IPS e.max® CAD LD glass-ceramic materials with different crystalline phases and thickness in different firing temperatures.
- 2) To investigate the optical properties as translucency parameters, contrast ratio, light transmissions and color changes of each translucent (high-translucent and low-translucent) IPS e.max® LD glass-ceramic materials with different crystalline phases and thickness in different firing temperatures.

- 3) To determine the mathematical relationships of thicknesses of IPS e.max® CAD LD glass-ceramic materials with TP and light transmission.

#### NULL HYPOTHESIS

1. Translucency parameters, contrast ratio, light transmissions and color changes between high-translucent and low-translucent IPS e.max® CAD LD materials with different thicknesses and different firing temperatures show no significant difference.
2. Translucency parameters, contrast ratio, light transmissions and color changes between different thicknesses and different firing temperatures of each translucent (high-translucent and low-translucent) IPS e.max® CAD LD materials show no significant difference.
3. The mathematical relationships of thicknesses of IPS e.max® CAD LD materials with the translucency parameters and light transmission follow a similar relationship.

#### ALTERNATIVE HYPOTHESIS

1. Translucency parameters (TP) light transmissions and color changes between high-translucent and low-translucent IPS e.max® CAD LD materials with different thicknesses and different firing temperatures show significant difference.
2. Translucency parameters, contrast ratio, light transmissions and color changes between different thicknesses and different firing temperatures of each translucent

(high-translucent and low translucent) IPS e.max® CAD LD materials show significant difference.

3. The mathematical relationships of thicknesses of IPS e.max® CAD LD materials with the translucency parameters and light transmission do not follow a similar relationship.

REVIEW OF LITERATURE

## DENTAL CERAMICS

The term ceramic is derived from the word “*keramos*” that means “pottery” in Greek. Ceramic is not a new material in dentistry. It was first introduced in dentistry in 1789, and the first ceramic crown was placed by Charles Land, a French dentist.<sup>13</sup> In general, this material is strong in compression while weak in tension, and brittle. In contrast, metal is a ductile material. The type of bond between the atoms is responsible for brittleness and ductility.<sup>14</sup> Ceramic consists of glass matrix and crystals. Glass is responsible for the optical quality, and crystals are responsible for the strength. The more glass contents the higher esthetics, the more crystals the stronger and opaque are ceramic. However, the glass phase is the weakest part, in which crack propagates<sup>15</sup> leading to the restoration failure. The properties of the ceramic count on the amount of crystals and glass content, interaction between them, crystals size, and processing technique.<sup>14, 16</sup> Etchability of ceramic is an advantage; it offers microretention for the adhesive to penetrate.

## DENTAL CERAMICS CLASSIFICATION

Fixed dental prostheses (FDP) can be divided into three main types of restorations according to their clinical applications: (1) all-metal, (2) metal-ceramic, and (3) all-ceramic.<sup>8</sup> The all-ceramic FDPs can be further classified into two classifications according to (a) microstructural phases or (b) fabricating techniques.<sup>9</sup> Based on microstructural phases, all-ceramic restorations can be subcategorized into four groups: (1) predominantly glass-based, (2) glassy-crystalline, and (3) crystalline-based

systems with glass fillers, (4) polycrystalline.<sup>9</sup> In addition, fabricating techniques class can be subcategorized into the four groups: (1) powder-liquid condensation, (2) slip casting, (3) heat-pressed, and (4) CAD-CAM machined.<sup>9,17</sup>

## A. MICROSTRUCTURAL PHASES

### A.1. Predominantly glass-based Ceramics

These dental ceramics are well described as the best material that mimics the optical properties of enamel and dentin.<sup>1</sup> Glass-based systems are made mainly of aluminosilicates glass which contain mainly: (1) silicon dioxide, which is known as silica or quartz, and (2) alumina (aluminum oxide). This glass is three-dimensional (3-D) networks of atoms with irregular regular pattern (distance and angle) between nearest or next nearest neighbors; thus, their structure is amorphous. Aluminosilicates can be found in nature with various amounts of potassium and sodium, and known as feldspars.<sup>1,18</sup> It has low flexural strength, ranges from 60 MPa to 70 MPa.<sup>19</sup> Thus, it can be used only as veneering material for metal or ceramic.

### A.2. Glass-based systems with fillers (glassy-crystalline)

This category of materials has a very large range of glass–crystalline ratios and crystal types. The glass composition is basically the same as the pure glass category. Thus, filler particles are added to the base glass composition to expand the clinical uses, which improve the mechanical properties, create a residual compressive stress within the

surface of the restoration, and control the optical properties as well.<sup>1, 19</sup> Fillers are mainly crystalline and result in different phases amount, which is known as composites to simplify this concept. Leucite is the most and first filler used for glass-based system. This filler was added to create porcelains to be compatible with metal substructure during firing. Thus, leucite fillers with 17-40 % mass can be added to glass-ceramic, which led to a higher thermal expansion than dental alloy to create porcelains that are thermally compatible during firing with dental alloys. This type of glass-ceramic is called Low-to-moderate leucite-containing feldspathic glass. Adding a high content of leucite particles (approximately 50% or higher) to the glass base ceramic improves the mechanical properties of the material and can be used as all-ceramic restoration. Leucite particles have an index of refraction that is very close to the feldspathic porcelain, which is very important to have high translucency result.<sup>1</sup> Also, leucite particles can be chemically etched in a faster rate than the feldspathic porcelain, which can improve the micromechanical bond of the all-ceramic restorations.<sup>1</sup>

#### A.2.1. Glass-ceramics (special subset of particle-filled glasses)

Glass-ceramics contain more than 50 vol.% of uniformly distributed crystals grown directly from the glass through a controlled nucleation and crystallization process and this includes two-stage heating treatment, which is called *ceraming*. The first heat treatment is called nucleation in which the mix powder is heated above the glass transition temperature to create maximum nuclei of the crystals. The second heat treatment is established at a higher temperature to initiate and then maximized the growth of the crystals to optimal diameters within the glass.<sup>19, 20</sup> The mechanical and optical



properties of the glass-ceramic materials depend on their crystal types, the crystal volume fractions, the nucleation and the crystallization rate, and the compatibility of the crystalline phases to the glass phases.<sup>19, 21</sup>

The first dental glass-ceramic was developed in 1972 by Grossman and marketed in 1984 under the trademark Dicor®. It was a fluormica glass-ceramic with a flexural strength of 150 MPa and consists of more than 55% volume fraction of small block-like tetrasilicic fluormica platelets (1–2 µm). Tetrasilicic mica glass-ceramic is produced from K<sub>2</sub>O–MgF<sub>2</sub>–MgO–SiO<sub>2</sub> glass system. Dicor® was first available as a castable glass-ceramic ingot for manufacture in the lab using the lost wax technique, and later as a machinable block.<sup>19, 20, 22</sup> Dicor® has multiple disadvantages that led to its discontinuity. Complicated lab work, low homogeneity during processing, poor margins fit, and the need for higher strength all-ceramic restoration make Dicor® discontinued. Thus, a new heat-pressable glass-ceramics were developed that exhibited higher strength and were easier to process in the dental lab.<sup>19</sup>

IPS Empress® was the first developed pressable glass-ceramic in 1986 with high leucite-containing glass-ceramic. Lucite-based glass-ceramic derived from the ternary phase system (SiO<sub>2</sub>–Al<sub>2</sub>O<sub>3</sub>–K<sub>2</sub>O system). It is the same ternary phase system with the feldspathic porcelain, but with higher content of K<sub>2</sub>O. It consists of a 35–45% volume fraction of randomly shaped 1–5 µm tetragonal leucite crystals and arranged like strings of beads along the glass grain boundaries.<sup>19, 20</sup> In 2004, the system was further expanded and optimized with the introduction of the new high translucent IPS Empress® Esthetic pressable ceramic. This was followed by the release of IPS Empress® CAD in 2006, creating an opportunity for this material to be milled using CAD-CAM technology at the

chairside. IPS Empress® Lucite-based glass-ceramic has a flexural strength of 160 MPa with excellent esthetic due to its high translucency. However, this material still exhibits insufficient strength to be used as posterior restorations, especially as a multiple unit restorations.<sup>19</sup>

Not until the first LD glass-ceramic restoration materials were introduced in dentistry in 1998 that we had a high flexure strength and high esthetic glass-ceramic restoration outcome. LD glass-ceramic material is discussed in details later in this review of literature.

### A.3. Crystalline-based systems with glass fillers

#### (Glass-infiltrated Oxide Ceramics)

The glass-infiltrated oxide ceramic framework consists of a porous pre-sintered ceramic core that is subsequently infiltrated with a low-viscosity glass. The ceramic core can be fabricated in the dental lab either by slip casting ceramic powder slurry on a porous refractory die, or by milling out from a pre-fabricated CAD-CAM ceramic block made by powder dry pressing.<sup>1, 8, 19, 23</sup> The oxide ceramic framework can be fabricated from different oxide materials and infiltrated by different glass materials. The available used oxide ceramics are aluminum oxide ( $\text{Al}_2\text{O}_3$ ), magnesium aluminum oxide ( $\text{MgAl}_2\text{O}_4$ ), and zirconium oxide ( $\text{ZrO}_2$ ). Glass-infiltrated Oxide Ceramics were first introduced in dentistry as In Ceram ® Alumina in 1989. It consists of 75 vol.% polycrystalline alumina and 25% infiltration glass with flexure strength of 400–500 MPa. Its high strength and medium translucency make it eligible to be used as anterior and posterior restorations.<sup>1, 8, 19, 23</sup> In 1994, In-Ceram® Spinell was introduced to overcome

the opacity of In-Ceram Alumina. The framework consists of 78 vol.% magnesium and aluminum oxide ( $\text{MgAl}_2\text{O}_4$ ), which improve the translucency of the material. This system is the highest esthetic in this category due to its high translucency, but it exhibits flexure strength of 350 MPa, which make it to be used mainly as an anterior all-ceramic restoration. In 1999, Zirconium oxide has been added to In-Ceram® Alumina to introduce In-Ceram® Zirconia as a new stronger material. In-Ceram® Zirconia consists of 56 vol.% polycrystalline alumina, 24 vol.% polycrystalline zirconia. This system is the strongest among this category, which exhibits a high strength of 700 MPa, and it is recommended to be used as single and multiple posterior unite FDP. As in the conventional In-Ceram technique, In-Ceram® Zirconia can be slip cast or milled from pre-sintered blocks, and is then glass infiltrated.<sup>1, 19, 23</sup>

#### A.4. Polycrystalline ceramics

Polycrystalline ceramics are solid-sintered monophase ceramics with no glassy components. Polycrystalline ceramics are formed by direct sintering crystals without any glass.<sup>1, 24, 25</sup> All atoms are densely packed into random arrays that are much more difficult to drive a crack through. Several processing techniques allow the fabrication of either solid-sintered aluminum oxide (alumina,  $\text{Al}_2\text{O}_3$ ) or zirconium oxide ( $\text{ZrO}_2$ ) framework. There are two methods of application for the polycrystalline ceramics. First, Aluminum oxide or zirconium oxide is pressed onto an oversized die and predictably shrunk during firing to become well-fitting, single-crown substructures. The second method is machining blocks of partially crystallized (10% complete) zirconium oxide into oversized greenware. The second method is easier and produce better margin fit restoration than the

first method. Recently, Polycrystalline zirconia ceramics are twice as strong and tough as polycrystalline alumina ceramics with a flexural strength range from approximately 900 MPa to 1100 MPa and fracture toughness between 8 MPa and 10 MPa. Thus, this material is a strongest and toughest available for dental all-ceramic restoration.<sup>1, 24, 25</sup>

## B. FABRICATING TECHNIQUES

### B.1. Powder- liquid condensation

Powder-liquid condensation technique is the most traditional and the simplest method for layering and veneering dental porcelain. This involves applying a moist porcelain powder with a special brush and removing excess moisture to get compact powder particles with less moisture. The porcelain is further compacted by viscous flow of the glass component during firing under vacuum pressure. This technique results in very translucent restoration with high esthetic result. However, a large amount of residual porosities can be a result of this technique because moistures are involved in the process and can cause varying degree porosities with less compact porcelain after drying and firing. Thus, these porosities can impact the strength and toughness of the restoration.<sup>1, 9,</sup>

26

### B.2. Slip cast

The process of slip casting uses both ceramic slips and glasses separately. It involves a two-step heat treatment. First, low viscosity slurry or a mixture of ceramic powder particles is suspended in water to make a slip. This slip is poured into a gypsum mold of a negative replica of an exact framework shape. This mold absorbs some water

and makes compact ceramic particles against the wall of the mold. Then, the ceramic particles are partially sintered before the framework removed from the mold. The resulting framework is porous and then it can be infiltrated and sintered again. The glass-infiltrated ceramic cores typically exhibit higher fracture resistance and strength than those fabricated by powder-liquid condensation because the strengthening crystalline particles form a continuous network throughout the framework.<sup>1, 9, 19, 26</sup>

### B.3. Heat-pressed

The heat-pressed process is a lost-wax casting method with using pressable ingots of crystalline particles distributed throughout a glassy material. After fabricating an exact replica of the final restoration with wax, the wax model is invested in a mold with gypsum materials. Then, the mold is heated to burn out the wax, leaving a cavity. In the pressing, a pressable ingot is heated to a temperature at which they become a highly viscous liquid, and they are slowly pressed into the lost wax mold. The resultant product can be finished either with the staining and used as an end product or cutback techniques and adding a layer of porcelain veneer for better esthetic result.<sup>1, 9, 19, 26</sup>

### B.4. Computer-Aided Design and Computer-Aided Manufacturing (CAD-CAM)

Computer Aided Design/Computer Aided Design (CAD-CAM) technology have been available for more than 20 years and was first introduced in dentistry by Duret.<sup>24</sup> CAD-CAM ceramic materials are available as prefabricated ingots. These ingots are milled by computer-controlled tools.<sup>9</sup> The technology started with milling fully sintered ceramic blocks, which is known as hard machining. It has then evolved to mill partially

sintered ceramics, which is known as soft machining. These are fully heat treated after milling to ensure adequate sintering.<sup>26</sup>

#### B.4.1. Hard Machining

Fully sintered ceramic materials available for CAD-CAM of dental restorations include feldspar-based, leucite-based and lithium disilicate-based ceramics.<sup>26</sup> Feldspar-based material has polygonal sanidine  $[(\text{Na}, \text{K}) \text{AlSi}_3\text{O}_8]$  crystals (2–10  $\mu\text{m}$  in diameter). A few microcracks usually present in this material due to some degree of thermal expansion mismatch between some of the crystals and the glassy matrix. The amount of crystalline phase in this material is about 30 vol. %.<sup>27</sup>

A leucite-reinforced ceramic is also available as machinable blocks for CAD-CAM restorations. This material is similar in microstructure and mechanical properties to the leucite-reinforced pressable ceramics. In general, machining of fully sintered ceramics result in significant tool wear and residual surface flaws that suppress the general physical performance of these materials.<sup>8, 28</sup>

Now a day, partially crystallized CAD-CAM LD glass-ceramic blocks are available to overcome the drawbacks fully crystallized ceramics machining. These materials are discussed in details later in this thesis.

#### B.4.2. Soft machining

This technology can be used to machine pre-sintered alumina, spinel, or zirconia-toughened-alumina blocks to fabricate FDP. The copings are further glass-infiltrated, resulting in a microstructure similar to that of slip-cast ceramics. The mechanical

properties of these materials are comparable to those of the slip-cast version, with a final marginal accuracy within 50  $\mu\text{m}$ . Soft-machining of partially sintered zirconia ceramic blocks by CAD-CAM technology was proposed in 2001.<sup>29</sup> The design compensates for the volume shrinkage of 25% that will later occur during sintering of the zirconia blocks. The partially sintered blocks are easy to mill, save time and decrease tool wear.<sup>8</sup> The type of zirconia used in this technology is mainly biomedical grade tetragonal zirconia stabilized with 3 mol % yttria. This material can be used as monolithic restoration or coping without glass infiltration and veneered with porcelain for better esthetic outcome.<sup>8</sup>

Hard machining is very useful for chair side single appointment restoration. However, the all-ceramic restoration of this technology is mainly used as single unit restoration due to its low to moderate strength. With the emerging of soft machining technology, all-ceramic restoration of this technology can be used safely for multi-unit restoration.<sup>8</sup>

## LITHIUM DISILICATE (LD) GLASS-CERAMICS

LD glass-ceramics were first introduced into dentistry in 1998 by Ivoclar Vivadent and it was marketed as IPS Empress® 2. It contains approximately 65-70% volume fraction of LD, 34% volume fraction of residual glass, and 1% volume fraction of porosity after heat treatments.<sup>30</sup> Unlike the binary LD system that was first developed by Stookey (1959)<sup>31</sup>, the IPS Empress® 2 was derived from a multi-component system, formulated from  $\text{SiO}_2\text{-Li}_2\text{O-K}_2\text{O-ZnO-Al}_2\text{O}_3\text{-La}_2\text{O}_3\text{-P}_2\text{O}_5$  compositions.<sup>20</sup> It has elongated crystals with a mean grain length and diameter of 5.2  $\mu\text{m}$  and 0.8  $\mu\text{m}$ .<sup>30</sup> IPS Empress® 2 then evolved to IPS e.max® press ingots in 2005. These ingots have been developed on the basis of the LD glass-ceramic and formulated from  $\text{SiO}_2\text{-Li}_2\text{O-K}_2\text{O-P}_2\text{O}_5\text{-Al}_2\text{O}_3\text{-ZrO}_2\text{-ZnO}$  system. IPS e.max® press has elongated crystals with a mean grain length and diameter approximately 3-6 $\mu\text{m}$  in length and 0.6-0.8 $\mu\text{m}$  diameters.<sup>20</sup> The ingots are produced by bulk casting which is a continuous manufacturing process based on glass technology (casting/pressing procedure). This new technology uses optimized processing parameters, which prevent the formation of defects in the bulk of the ingot.<sup>20, 32</sup> According to the manufacturer, IPS e.max® Press has a flexural strength of 400MPa and a fracture toughness of 3.0 MPa.

With the emerging of digital dentistry in computer aided design and especially computer aided manufacturing milling fabrication technique, a multicomponent glass-ceramic blocks such as IPS e.max® CAD were utilized in 2006 for the benefits of milling, increase cutting efficiency, and maximize the life of the milling tools.<sup>11, 12</sup>



Generally, IPS e.max® CAD restorations have three fabricating procedures: industrial casting of the blocks, CAD milling, and final thermal refinement so called crystallization.<sup>11</sup> The first processing, according to the manufacturer, glass compositions (mainly SiO<sub>2</sub>, Li<sub>2</sub>O, P<sub>2</sub>O<sub>5</sub>, ZrO<sub>2</sub>, ZnO, K<sub>2</sub>O, and Al<sub>2</sub>O<sub>3</sub>) are incongruently melted, quenched, and annealed to form blue ingots by polyvalent coloring elements.<sup>33</sup> These are partially crystallized lithium metasilicate blocks that have enough strength and hardness to make it easy to be milled by a CAD-CAM system, which is the second process.<sup>33</sup> Finally, the milled block goes through the heating schedule for crystallization of LD.<sup>11</sup>

#### MICROSTRUCTURE OF IPS E.MAX® CAD LITHIUM DISILICATE

The microstructure of the partially crystallized blocks consists of 40% lithium metasilicate crystals (Li<sub>2</sub>SiO<sub>3</sub>), which are embedded in a glassy phase with grain size of the platelet-shaped crystals of range between 0.2 to 1.5 μm and exhibits a flexural strength of 130 +/- 30 MPa. The final crystallized material consists of 65-70% fine-grain LD crystals (Li<sub>2</sub>Si<sub>2</sub>O<sub>5</sub>), which are embedded in a glassy matrix and the strength increases to 360 MPa and a fracture toughness of 2.25 MPa.<sup>8, 11, 12, 26</sup>

In today's dental market, IPS e.max® CAD material can be available in two levels of translucency as high-translucent (HT) and low-translucent (LT) material depending on their microstructural component. Depending on the crystallization pre-treatment of the ceramic blocks, these two levels of translucency can be obtained. The HT material contains fewer and larger crystals of lithium metasilicate in the pre-crystallized state while the LT material contains a higher density of smaller crystals.

After full crystallization heat treatment, the HT ceramic has layered  $\text{Li}_2\text{Si}_2\text{O}_5$  crystals ( $1.5 \times 0.8 \mu\text{m}$ ) in a glassy matrix. Highly soluble  $\text{Li}_3\text{PO}_4$  spherical crystals appear as spherical pores. The fully crystallized LT ceramic exhibits a high density of small ( $0.8 \times 0.2 \mu\text{m}$ ) interlocked  $\text{Li}_2\text{Si}_2\text{O}_5$ , together with spherical pores, also interpreted as  $\text{Li}_3\text{PO}_4$  crystals.<sup>8, 26</sup>

## THE EFFECT OF TREATMENT OF LITHIUM DISILICATE

### GLASS- CERAMICS

The microstructure behaviors of the LD glass-ceramics are dependent on its thermal history and it is not new to the existing literature. The growth of LD crystals can be affected by a one- or two-stage heating schedule.<sup>34-36</sup> The one-stage heating schedule included a single heating rate and holding time. On the other hand, the two-stage heating schedule involved first and second heat treatments for nucleation then crystallization, respectively. The initial heat-treatment stage is important to establish a kinetically favorable setting for stabilizing lithium metasilicates. The second heat-treatment stage always at a higher temperature range than the initial, supplied the thermal energy to induce growth and maturation of LD and to destabilize the lithium metasilicates.<sup>35</sup> Past investigations have argued that a two-stage heating schedule precipitated more mature and larger LD crystals than a single-stage heating schedule. Although, the single-stage heating schedule might require less overall processing time, it seemed to lack the appropriate thermal enrichment of maturation of LD crystals.<sup>34-36</sup>

## PHASE FORMATION SEQUENCES IN LITHIUM DISILICATE GLASS-CERAMICS

The nucleation, crystallization, and phase formation and transformations of the multicomponent LD glass-ceramic materials have been recently dramatically investigated and analyzed.<sup>7, 34, 36-40</sup> The phase evolution in the multicomponent LD glass-ceramic material over temperature can be divided into several periods; induction period, nucleation of lithium metasilicate ( $\text{Li}_2\text{SiO}_3$ ) and LD ( $\text{Li}_2\text{Si}_2\text{O}_5$ ) period, saturated nucleation period,  $\text{Li}_2\text{SiO}_3$  to  $\text{Li}_2\text{Si}_2\text{O}_5$  transformation period, crystal growth of  $\text{Li}_2\text{Si}_2\text{O}_5$  and lithium phosphate ( $\text{Li}_3\text{PO}_4$ ), melting period of  $\text{Li}_2\text{Si}_2\text{O}_5$ , and melting period of  $\text{Li}_3\text{PO}_4$ .<sup>34, 37-40</sup> The postulated phase formation sequences in the LD glass changes that occur during firing temperature variations according to Huang et al., 2013 are shown in Table 1.<sup>38</sup>

In general, at a temperature above 520 °C, the crystallization of  $\text{Li}_2\text{SiO}_3$  starts and reaches its maximum at 750 °C and dissolved above 780 °C.<sup>37-39, 41</sup> It is accompanied by the crystallization of initially formed  $\text{Li}_2\text{Si}_2\text{O}_5$ .  $\text{Li}_2\text{Si}_2\text{O}_5$  remains very low starting from 580 °C up to a temperature of approximately 750 °C at which the  $\text{Li}_2\text{Si}_2\text{O}_5$  is dramatically growing and reaches to a maximum crystal saturation at 820 °C before its maturation.<sup>38</sup> After this vigorous growth and maturation of  $\text{Li}_2\text{Si}_2\text{O}_5$ , it reaches its maximum maturation and size at a temperature of 840 °C, which consist of 65-70% fine-grain LD crystals ( $\text{Li}_2\text{Si}_2\text{O}_5$ ).<sup>19, 41</sup> At this temperature, the IPS e.max CAD material heating stops. By continuing raising the heating temperature, the  $\text{Li}_2\text{Si}_2\text{O}_5$  melts at a temperature of 950 °C and the whole glass content melts at a temperature of 1010 °C.<sup>38</sup>

## IPS E.MAX CAD BLOCKS FABRICATION AND FINAL CRYSTALLIZATION

The industrial casting of IPS e.max® CAD blocks are based on the behavior of the nucleation, crystallization, and phase formation and transformations of the multicomponent LD glass-ceramic system. The glass materials (mainly SiO<sub>2</sub>, Li<sub>2</sub>O, P<sub>2</sub>O<sub>5</sub>, ZrO<sub>2</sub>, ZnO, and K<sub>2</sub>O) are melted in a temperature of 1300 to 1600° C for 2 to 10 hours. Then, the parent glass is formed into glass blocks by pressure casting into a steel mold. Before cooling down to the room temperature, the melted glass is transferred into a pre-heated furnace in 500 to 600° C for a period of about 10 minutes to 3 hours to relax the glass block and avoid stress build-ups in the glass. This results in a formation of a great number of nuclei to ensure efficient crystal growth of Li<sub>2</sub>SiO<sub>3</sub>. In addition, the glass block is heated at a temperature of 690–710°C for 10–30 min to form Li<sub>2</sub>Si<sub>2</sub>O<sub>5</sub> crystals grown epitaxially from the Li<sub>3</sub>PO<sub>4</sub> nuclei and cooled down to the room temperature. The final product is marketed in blue color block to be used for CAD dental restoration, which contains Li<sub>2</sub>SiO<sub>3</sub> ~40% and ~60% glass phase.<sup>19, 33</sup> The manufacturer recommends crystallization process consists of two heating rates and two holding times. Initially, the partially crystallized precursor is heated at a rapid rate of 90 °C/min from 403 °C (furnace stand-by-temperature) to 820 °C and held for 10 seconds at 820 °C (first targeted temperature). This is followed by a slower, second heating rate of 30 °C/min. Then, it is held for a prolonged period of seven minutes at 840 °C (second targeted temperature).<sup>6</sup>

## LIGHT AND COLOR

Light is a form of energy and composed of different wavelengths. When the light exposed to an object, the light could be reflected at the surface of the object (specular or diffuse), and it could be absorbed or scattered within the object, or it could refract or totally transmitted through the object.<sup>42, 43</sup> The wavelengths (colors) that are reflected, refracted or transmitted are perceived by receptor cells (i.e. rods and cones) in the eye and recognized by the brain as a specific color. The wavelengths of visible light range from approximately 400 to 700 nm.<sup>43, 44</sup> The wavelengths that are transmitted, refracted or reflected create the color that is perceived and till about the translucency level of the material. If all light is transmitted, the material appears completely transparent. If all light is absorbed, the material appears completely opaque, and the color black is perceived. However, if some of the wavelengths of the visible light are absorbed and others reflected, refracted, or transmitted, the color that is perceived corresponds to the wavelengths that are reflected, refracted, or transmitted, and the level of translucency depends on the amount of the light that transmitted through the material.<sup>8, 42-44</sup> Moreover, the reflection of the light depends on the surface texture of the restoration. Thus, a smooth surface increases the specular reflectance, in which the angulation of light reflection is equal to the angle of the light source. This reveals more of the color of the light than the color of the restoration, which appears saturated in color.<sup>8, 42-44</sup> However, the light scatters in many different directions when the surface is rough. This is known as diffuse reflectance, which reveals more of the object's color and appears less saturated and duller in color.<sup>45</sup>

Correct light intensity and the proper illuminants illumination are essential for color evaluation. Since 1931, the light source used as the standard daylight was C, incandescent or tungsten lamps (2856 K), or fluorescent lamps (4000 K). Currently, an average standard daylight is D65 and D55. Illuminant D65 and D55 refer to the correlated color temperatures of 6500 K and 5000 K, respectively.<sup>43,44</sup> D65 was defined in 1964 as the radiation of north sky daylight on a cloudy day. According to ISO 3668 and 3664, D65 is the standard application used in the industries, while D55 is used in the printing and graphic arts industries.<sup>43,44</sup>

Color systems are used to describe the color parameters of objects. Munsell color system is the oldest color order system and has been used in dentistry. The Munsell color system uses a three-dimensional system with hue, value, and chroma as coordinates. The value (V) represents the color lightness or darkness, ranging from 0 (black) to 10 (white). Munsell chroma (C) represents the saturation of a particular hue and it is an open-ended scale ranging from achromatic colors to a maximum depending on the hues. Also, Munsell hue (H) is commonly referred as color (e.g. red, orange, green, and blue). Hue is also associated with the wavelengths of the light observed.<sup>8,42,43</sup>

The Commission Internationale de l'Eclairage (CIE, International Commission on Illumination) developed another commonly used color specification system. The CIE tristimulus value system uses three parameters, X, Y, and Z, which are based on the spectral response functions defined by the CIE observer. Another CIE color system (CIE L\*a\*b\*) uses the three parameters L\*, a\*, and b\* to define color.<sup>8,42,</sup>

<sup>43</sup> The L\*, a\*, and b\* values can be calculated from the tristimulus X, Y, and Z values

and vice versa. This color system is an approximately uniform three-dimensional color space whose elements are equally spaced on the basis of visual color perception. The quality  $L^*$  represents lightness and ranging from 0 (black)-100 (white), whereas chroma ( $a^*b^*$ ) is denoted as red ( $+a^*$ ), green ( $-a^*$ ), yellow ( $+b^*$ ), and blue ( $-b^*$ ).<sup>8, 42, 43</sup>

The color of the LD glass-ceramics is controlled by coloring ions that are dissolved in the glass matrix. The color depends on the valency of the ions and the field surrounding the ions. In lithium LD glass-ceramic, the primary ions are  $V^{+4} / V^{+3}$  (blue/yellow),  $Ce^{+4}$  (yellow), and  $Mn^{+3}$  (brownish). For the IPS e.max CAD material, the vanadium (V) is in a valency of +4 due to the surrounding state conveyed by the lithium metasilicate crystals. After milling and during the heat treatment, the primary crystal structure changes from lithium metasilicate to LD, the valency of the vanadium changes from  $V^{+4}$  to  $V^{+3}$  and the color given for these changes from blue to yellow. As the final color is a result of the concentration of ions and the influence of the matrix glass, controlling the melting conditions of the blocks are essential.<sup>46</sup>

## TRANSLUCENCY AND LIGHT TRANSMISSION

Translucency is an important factor to control the esthetic outcome of any dental ceramics.<sup>47</sup> Translucency is a property of materials that allow the light to pass through the material, but disperses the light, so no objects can be seen through the material.<sup>8, 43, 44</sup> The greater the quantity of light that passes through the object, the higher the translucency of the material.<sup>8</sup> The highest translucency is transparency, in which all light is transmitted, while the lowest is opacity, in which all light is reflected or absorbed.<sup>43, 44</sup>

In general, all-ceramic systems have different compositions, microstructure, crystalline content phases, processing technique, and the material thickness and shade, which influence the optical and mechanical properties of these systems. In addition, the amount, shape and particle size distribution of the crystalline phase and porosity directly also influence the mechanical and optical properties of ceramic material.<sup>3, 48, 49</sup> Thus, higher the crystalline content, the higher strength and lower translucency.<sup>8</sup> For example, IPS e.max® CAD system is a LD glass-ceramic ( $\text{Li}_2\text{Si}_2\text{O}_5$ ) with a crystalline content of about 65-70% and a flexural strength of 360 MPa. However, IPS Empress® CAD is a Leucite-reinforced glass-ceramics ( $\text{KAlSi}_2\text{O}_6$ ) with a crystalline content of about 35% and a flexural strength of about 160 MPa.<sup>8</sup> In addition, the crystal size can influence the translucency of the material in a different prospective. As mentioned earlier, IPS e.max® CAD has HT and LT. Both have the same crystal content and flexure strength, but they are different in crystal sizes. HT ceramic exhibits crystals of 1.5 x 0.8 mm in a glassy matrix, whereas LT ceramic exhibits smaller crystals (0.8 x 0.2 mm) interlocked in a high density matrix.<sup>26</sup> Moreover, different crystalline compositions in different ceramics types show different translucency levels.<sup>3</sup> However, the translucency of dental ceramics could be also affected by thickness regardless the ceramic composition. As the ceramic thickness decreases the translucency increases.<sup>50, 51</sup> Also, The higher the amount of remaining void, the more scattering and lower light transmittance.<sup>48</sup>

Furthermore, the translucency of the IPS e.max® CAD LD glass-ceramic material is controlled by the nanostructure of the material. Scattering of light at the interfaces between the crystals and the glass matrix causes is the key point for the translucency properties.<sup>52</sup> If there is a similar refractive index of light between the crystals and the



glass matrix, such as between the LD crystals and the glass matrix, it is possible to achieve a very high translucency. If the difference in refractive index between the crystals and the glass is high, then low light passes through the material and low translucency results.<sup>52</sup> Thus, different translucencies are used for a variety of different applications to produce translucencies that are well accepted within the industry. As claimed by manufacturer, The manufacturing processes used to control translucency have no influence on the mechanical properties such as the strength and modulus of the material.<sup>46</sup>

There are two forms of transmittance (specular and diffuse) and each one depends upon the method of measurement. In the diffuse transmittance, the measurement includes all the light passing through the material and all the light scattered in a forward direction, and this is known as specular component included (SCI). For the specular transmittance, the measurement excludes the proportion of scattered light that does not reach the detector, and this known as specular component excluded (SCE).<sup>48, 53</sup>

Several methods have been reported in the literature to investigate the translucency of the restorative materials, such as: the translucency parameter (TP),<sup>47, 51, 54-56</sup> contrast ratio (CR),<sup>3, 47, 57-60</sup> and transmittance of light.<sup>47, 59, 61, 62</sup>

The translucency parameter (TP) was first introduced to evaluate the translucency of maxillofacial elastomer.<sup>54</sup> TP is a standardized method to calculate translucency considering the entire visible spectrum. The TP is defined as the color difference between a material of uniform thickness over a white and a black background.<sup>54</sup> The quantitative measurement of translucency is obtained by comparing the reflectance of light through the samples over a background with high reflectance (white background) to that of

high absorbance (black background). The recorded measurement is a result of the light that is reflected back to the measuring device by the background, after being transmitted through the samples.<sup>54</sup> The TP values are calculated by using the following equation:

$$TP = \sqrt{(L_b^* - L_w^*)^2 + (a_b^* - a_w^*)^2 + (b_b^* - b_w^*)^2} \quad (1)$$

The  $L^*$  values of 0 to 100 represent the measure of the lightness or darkness of the material.<sup>43</sup> The  $a^*$  values represent the measure of redness or greenness, and the  $b^*$  values represent that of yellowness or blueness.<sup>43</sup> Positive  $a^*$  relates to the amount of redness, and negative values relate to the greenness of the samples, whereas positive  $b^*$  values relate to the amount of yellowness and negative values relate to the blueness of the sample.<sup>63</sup> The subscripts refer to the color coordinates on the black background ( $b$ ) and ( $w$ ) to those on the white background. A high TP value indicates high translucency and low opacity and vice versa.<sup>47, 51, 54, 55</sup>

In 1987, Powers et al. used contrast ratio (CR) to measure the translucency of restorative resin.<sup>57</sup> CR is the ratio of the reflectance that obtained from an object resting on a black background to the reflectance obtained for the same material against a white background.<sup>43, 57, 58</sup>

The CR values are calculated based on the following equation:

$$CR = \frac{Y_b}{Y_w} \quad (2)$$

$Y_b$  represents the spectral reflectance of the light of the sample on a black background and  $Y_w$  on a white background. The value of a completely transparent material is 0, while the value of a completely opaque material is 1.<sup>43, 47, 57, 58</sup> Y value can be calculated from  $L^*$ . Since Y is luminance from Tristimulus Color Space CIE XYZ, Y can be calculated from

the following equation:<sup>47, 64</sup>

$$Y = \left( \frac{L^*+16}{116} \right)^3 \times Y_n \quad (3)$$

For simulated object colors, the specified white stimulus normally chosen is one that has the appearance of a perfect reflecting diffuser, normalized by a common factor so that  $Y_n$  is equal to 100.<sup>65</sup>

Moreover, LD glass-ceramic can be used as either all-ceramic full coverage FDP (e.g. crown and bridge) or partially coverage indirect FDP (e.g. inlay, onlay, and veneers). Resin cements are most common cements used for such kind of restorations. Resin cement is available as chemical polymerized, photo polymerized or a combination of both. Resin cement has an ability to bond to the restoration and the tooth as well. It has superior optical properties and it is available in different shade and translucencies<sup>66</sup>. However, incomplete polymerization of resin cement can result in degradation of the cement, staining around the restoration margin, debonding of the restoration, and possible pulp irritation due to the residual unreacted monomer.<sup>48, 66</sup>

Furthermore, chemically polymerized systems are mainly used under low translucent or thick restoration materials, due to the low light intensity that can pass through the material. Photo (light) polymerized systems are mainly indicated for translucent veneers, due to the possibility of light transmission through the restoration material. Dual- polymerized systems can be used in either situation, since the chemical activation of dual cements could compensate for the low light intensity that can reach to the resin cement.<sup>48, 66, 67</sup> The light intensity that reaches the cement varies according to the optical characteristics of the restorative material.

## INSTRUMENTAL MEASUREMENT FOR COLOR AND TRANSLUCENCY

Various instruments can be used to measure color and translucency of dental materials, such as spectrophotometers, spectroradiometers or colorimeters.

### 1. Spectrophotometer

Spectrophotometers are widely used to measure surface colors. It is designed to measure the ratio of the light reflectance and based on the CIE system.<sup>43</sup> Spectrophotometers have the ability to analyze the principal components of a series of spectra and convert spectrophotometric measures to various colors measures.<sup>43, 68</sup> The result is quite stable and accurate as an absolute standard.<sup>43</sup>

### 2. Spectroradiometer

Spectroradiometer is an alternative to spectrophotometers to measure color in dentistry. They measure radiometric quantities: irradiance ( $\text{W}/\text{m}^2$ ) and radiance ( $\text{m}^2\text{Sr}$ ).<sup>43</sup> Their units are expressed by luminance ( $\text{cd}/\text{m}^2$ ) and illuminance (lux) for spectral radiance and irradiance, respectively.<sup>43</sup> There is a significant difference between the TP values measured by Spectroradiometers and Spectrophotometers. However, the measurements were very correlated.<sup>69</sup>

### 3. Colorimeter

Colorimeters measure color tristimulus values from light reflectance of a sample

after the light source has passed through a series of filters. These devices measure color only in terms of tristimulus according to CIE illuminant and observer conditions. Colorimeters use photodiode filters to control light reaching the sample.<sup>43, 68</sup> Colorimeters are useful in quantifying color differences between two samples. It is very simple for quantification of the optical properties of esthetic dental materials.<sup>43, 68</sup> However, Colorimeters are not registering spectral reflectance and can be less accurate than spectrophotometers due to aging of filters, and object metamerism can be a challenge to their accuracy.<sup>70, 71</sup>

## CURRENT CHALLENGES

The optical properties of ceramic materials include color and translucency in addition to hue, value and chroma.<sup>72</sup> All-ceramic systems have various compositions with different crystalline content, which may affect the optical properties of these systems.<sup>72, 73</sup> An increase in the crystalline content to achieve greater strength generally results in greater opacity and effect on the translucency, light transmission, and color.<sup>73</sup> The optical properties as translucency parameter (TP), contrast ratio (CT), light transmission parameter (Lt), and color changes (CC) of the multicomponent CAD-CAM LD glass-ceramic materials with different thicknesses have been investigated in the literature.<sup>56, 60, 61, 67, 74</sup> However, most of the optical property studies of the CAD-CAM LD glass-ceramics are mainly focused on the fully crystallized final product. Thus, the optical property studies of the CAD-CAM LD glass-ceramic materials in the partially crystallized and in different crystallization phases are very limited in the literature. Moreover, the TP, CR and Lt of this material with different thicknesses have been

reported separately in different studies with different samples preparations and methods. For this reason, it was essential to investigate the TP, CR, Lt of LD glass-ceramic material in our study with different thicknesses to standardize the methods and sample preparations to obtain results that can be statistically reliable. Also, the previous studies lack of show an incremental increase of the thicknesses, which is very important to determine a mathematical relationship between different thicknesses of IPS e.max® CAD LD glass-ceramic materials with TP and Lt. In addition, there is a lack of information in the literature about the comparison of TP, CR and Lt between the LH and LT IPS e.max CAD LD glass-ceramic materials. Also, there is a lack of information regarding the correlation between the optical properties of this material.

Moreover, the optical properties of the multicomponent LD glass-ceramic materials can reveal more about the behavior of these materials, especially during the transformation phase of the  $\text{Li}_2\text{SiO}_3$  to  $\text{Li}_2\text{Si}_2\text{O}_5$ . In addition, the microstructure of the multicomponent LD glass-ceramics has a direct effect on the optical properties. During this transformation phase of IPS e.max® CAD, the color of the block changes from the blue to the yellow color. In addition, the crystallization growth of  $\text{Li}_2\text{Si}_2\text{O}_5$  dramatically increases to a maximum, which cause changes in the translucency, light transmission and color of the material due to this growth.<sup>11</sup> Thus, one of our interests in this study was to investigate the optical properties as TP, CR, Lt and CC in three microstructure transformation phases, which are the beginning of the transformation of  $\text{Li}_2\text{SiO}_3$  to  $\text{Li}_2\text{Si}_2\text{O}_5$  at 750 °C, the complete transformation of  $\text{Li}_2\text{SiO}_3$  to  $\text{Li}_2\text{Si}_2\text{O}_5$  at 820°C and the complete maturation and crystallization of  $\text{Li}_2\text{Si}_2\text{O}_5$  at 840 °C. Also, we investigated the

color changes from the blue blocks to the final crystallized color in different firing temperatures.

In this study, we were investigated the optical properties as translucency parameter (TP), contrast ratio (CR), light transmission (Lt) and color change (CC) of two different translucent levels of IPS e.max® CAD LD glass-ceramic materials (HT and LT) with thicknesses in different firing stages. Furthermore, the TP CR, and Lt have been investigated and reported in samples of varying thicknesses in the past. However, no relation between the TP, Lt and thickness has been reported. In this study, we were also determined the mathematical relationship between TP and Lt with the thicknesses to correlate those parameters. Finally, we investigated the correlation between the TP, CR and Lt of IPS e.max® CAD LD glass-ceramic materials.

## MATERIALS AND METHODS



## MATERIALS

The materials that were used in this study are IPS e.max® CAD blocks (Ivoclar Vivadent, Liechtenstein, Germany). Two levels of translucency were used, which are high translucent blocks (HT) and low-translucent blocks (LT)<sup>11</sup>. Only one shade was used, which is A2.

## SAMPLE PREPARATIONS

Partially crystallized (blue state) shade A2 ceramic blocks (IPS e.max® CAD, Ivoclar Vivadent) were sectioned into square shape samples (15.25 mm X 15.25 mm) and five different thicknesses the thickness (1.00, 1.25, 1.5, 1.75, 2.00mm) (n=120) by using a diamond saw (Isomet 1000, Buehler, Lake Forest, IL) (Fig 1). Thickness of the samples was measured using a Vernier caliper with digital readout (Mitutoyo Corp., Tokyo, Japan). Both surfaces of the samples were polished using silicon carbide paper of 600-, 800-, 1000-, and 1200-grit (EXAKT Technologies, Oklahoma City, OK, USA) under running water at 300 rpm on a polishing machine (EXAKT 400 CS, EXAKT Technologies, Oklahoma City, OK, USA). The square samples were then equally divided into two main groups according to the translucency (HT/LT)(n= 60). Each group was divided into five main subgroups according to the thickness (1.00, 1.25, 1.5, 1.75, 2.00mm) (n=12). Each subgroup was divided into three further subgroups according to heating schedules (three different crystallization temperatures)(n=4) as 750 °C, 820 °C in

single stage heating schedule with 1 second and 10 second holding times, respectively, and 840 °C with two-stage heating schedule (820°C, 840 °C with 10 second and 7 min holding time, respectively, as recommended by manufacturer) by using Ivoclar Vivadent ceramic furnace (Programat® CS) (Fig 2,3) (Table II). After firing, both surfaces of the samples were polished using silicon carbide 1200-grit (EXAKT Technologies, Oklahoma City, OK, USA) under running water at 300 rpm on a polishing machine (EXAKT 400 CS, EXAKT Technologies, Oklahoma City, OK, USA). After polishing, the samples were rinsed with water and the thicknesses were verified using a Vernier caliper with digital readout (Mitutoyo Corp., Tokyo, Japan) in each thickness at the center of the disk with the variation at  $\pm 0.06$  mm (Fig 4). The samples were stored dry until testing performed (Fig 5).

#### TRANSLUCENCY AND COLOR CHANGE MEASUREMENT

The color space by CIE ( $L^*$ ,  $a^*$  and  $b^*$ ) of all samples was measured by a spectrophotometer (CM-2600D, Konica Minolta Sensing Americas, Inc., Ramsey, NJ) (Fig 6). The standard of device was controlled at a 10-percent observer angle, a 100-percent UV and standard illuminant D65 as the standard wavelength between 300 nm to 780 nm. The light reflected on the surface of samples through an 8-mm target mask Irradiance was measured with the ceramic discs of 1 mm, 1.25 mm, 1.5 mm, 1.75 mm and 2 mm thickness inserted underneath a spectrophotometer device on either a white or a black background (Fig 7). The data with specular component included and excluded (SCI and SCE) were recorded to compare the effect of surface roughness.

The translucency parameter was calculated from the differences between the color reflectance data of the white and black, according to equation (1).<sup>54</sup> The contrast ration (CR) was obtained by equation (2) after calculating Y value from equation (3).

## LIGHT TRANSMISSION MEASUREMENT

Managing Accurate Resin Curing (MARC® Resin Calibrator, BlueLight Analytics, Inc., Halifax, NS, Canada) (Fig 8) consists of a laboratory grade UV-VIS spectrometer and two-laboratory grade cosine corrected sensors (top and bottom). Light captured by the sensors is transmitted to the spectrometer through a bifurcated fiber optic cable, after which dedicated software provides real-time irradiance data. The MARC® Resin Calibrator was set to monitor the polymerizing time for 20 seconds and the sensor trigger at 11. Irradiance and spectra of the halogen light-curing unit (Optilux Demetron 401, Kerr, CA, USA) was measured in the standard mode. Irradiance were measured at a distance of 0 mm with the ceramic disks from each sample was inserted between the light curing unit and a radiometer device, MARC® Resin Calibrator (Fig 9).<sup>75</sup> The mean irradiance and the peak wavelength of the light-curing unit were measured by the top sensor, and determined to be  $922 \text{ mW/cm}^2$  and 488 nm, respectively (Fig 10).

## STATISTICAL ANALYSIS

The statistical methods include statistical analysis on outcomes: TP SCI, TP SCE, Mean Irradiance, Max Irradiance, Spectral Peak, SCI L\*, SCI a\*, SCI b\*, SCE L\*, SCE a\* and SCE b\*. For each outcome, the test results (mean, stand deviation, range) were summarized by Translucency, Firing Temperature and Thickness. The effects of the test results were evaluated using 3-way ANOVA with factors for Translucency (HT and LT), Firing Temperature (750, 850, and Rec) and Thickness (1, 1.25, 1.5, 1.75, and 2), as well as all two-way and three-way interactions among the factors. Pair-wise comparisons were made using Least Significant Differences to control the overall significance level at 5% (only the significant interactions were included).

Linear regression models were fitted by translucency and firing temperature using thickness as a continuous variable to exam the relationships between translucency and firing temperature, thickness and outcomes: TP SCI, TP SCE, Mean Irradiance, and Spectral Peak.

## RESULTS AND DISCUSSION

## RESULT ON MEAN IRRADIANCE

We performed 2-way ANOVA statically analysis on mean irradiance with  $p < 0.05$ . All Pairwise Multiple Comparison Procedures (Holm-Sidak method) show the overall significance level = 0.05 (Table III, IV).

The mean irradiance for the HT group at the recommended temperature decreases from 331.77 mW/cm<sup>2</sup> to 188 mW/cm<sup>2</sup> as the thickness increases from 1 to 2mm. The mean irradiance for the LT group decreases from 276.2 mW/cm<sup>2</sup> to 121.17 mW/cm<sup>2</sup> as the thickness increase from 1 to 2. There is statistically significant difference between the thickness groups within the HT group and the same observation is seen in the LT group (Fig 11). The result is expected since the higher material thickness absorbs more light and result in lower light transmission. More importantly, there is a statistically significant difference between the HT group and the LT group in all thickness groups, which is indicating a fundament difference in the light transmission between two materials and is discussed later in this thesis (Table V, VI).

Many authors have studied the effect of sample thickness on optical properties on ceramic materials.<sup>51, 55, 59-61</sup> Also, many authors propose a regression analysis based on Beer-Lambert law. However, the physical meaning of the regression parameters has never been fully explained.<sup>51, 76</sup>

Based on Beer-Lambert law, given a flat surface of IPS e.max® CAD sample which receives an incident irradiance ( $I_0$ ) normal to the surface, if the total reflected irradiance is ( $I_r$ ), then the irradiance immediately subsurface may be simply expressed by ( $I_0 - I_r$ ). If IPS e.max® CAD sample may be assumed to have a constant thickness ( $l$ ), then after attenuation by absorption and/or scattering throughout depth ( $l$ ) of the sample, the emergent light may be said to have a transmitted irradiance ( $I$ ). In practice, the light-irradiance  $I_0$  and  $I$  may be measured experimentally. One can define ‘true’ and ‘apparent’ quantities, as follows, where the latter does not take account of reflected light:<sup>77</sup>

$$\text{Apparent transmittance, } T_a = I/I_0 \quad (4)$$

$$\text{True transmittance, } T = I/(I_0 - I_r) \quad (5)$$

$$\text{Apparent absorbance, } A_a = \log_{10} \left( 1/T_a \right) \quad (6)$$

$$\text{True absorbance, } A = \log_{10} \left( 1/T \right) \quad (7)$$

However, the reflected light intensity cannot be easily defined. Here we propose a new approach based on the original Beer-Lambert law:

$$I/I_e = e^{-cl} \quad (8)$$

$I$  is the mean irradiance measured at any thickness

$I_e$  is the effective incidence irradiance when the sample thickness approach 0.

$c$  is the coefficient of absorption.

$l$  is the thickness of the sample.

By measuring the irradiance behind samples from multiple thicknesses a logarithmic plot between the irradiance and the samples thickness can be obtained. Through regression analysis, the y intercept of the regression and the slope of the curve can be obtained as well. From the y intercept, we can define the  $I_e$  that represents the effective incident irradiance, accounting for the reflectance as described by Watts and Cash.<sup>77</sup>

$$I_e = I_0 - I_r \quad (9)$$

The coefficients of absorption ( $c$ ) and  $I_e$  of the HT and LT groups were calculated for all firing temperature groups (Fig 12, 13). The result of coefficients of absorption ( $c$ ) and  $I_e$  are summarized in tables (Table VII, VIII) (Fig 14). There is no difference in the coefficients of absorption between the HT and LT at 750 °C and 820 °C. However, there are significant higher coefficients of absorption in the HT group compared to the LT group at the recommended temperature (Table IX). The result indicates that the differences between the coefficients of absorption of the HT and LT relate to the difference of LD crystals formed at the recommended temperature.

Regarding the spectral peak, there is an unexpected shift of the spectral peak from lower to higher wavelength as the thickness decreases in the 750°C and 820°C groups. However, this significant shift is not observed in the recommended group (Fig 15, 16) (Tab X, XI). Moreover, by analyzing the CIE  $L^*a^*b^*$  for all three firing temperatures, there is an obvious shift  $a^*$  and  $b^*$  value but not in the  $L^*$  (Fig 17). The shift in  $a^*$  value indicates the change from red to green. In addition, the large change in  $b^*$  from 750°C to the recommended temperature indicates a large shift from blue to yellow (Fig 18, 19). Our results show that the green and blue colors for the 750 °C and 820 °C groups have a



stronger impact on filtering the higher wavelengths, allowing only shorter wavelengths to pass through. Therefore the spectral peak shifts from low to high wavelengths of the samples when thickness increases for 750°C and 820°C groups. However, after the color change occurs in the recommended temperature group to more red and yellow, the filtering effect by the difference thicknesses disappears (Fig 18, 19)

## RESULT ON TP SCI

We performed 2-way ANOVA statistical analysis on TP that calculated from SCI with  $p < 0.05$ . All Pairwise Multiple Comparison Procedures (Holm-Sidak method) show the overall significance level = 0.05. (Table XXIV, XXV).

The TP for the HT group for the recommended temperature decreases from 22.47 to 13.05 as the thickness increases from 1 to 2mm. Also, the TP for the LT group decrease from 19.18 to 10.16 as the thickness increases from 1 to 2 (Fig 20). There is a statistically significant difference between the thickness groups within the HT group and the same observation is seen in the LT group (Table XXVI, XXVII). The result is expected since the higher material thickness absorbs more lights and result in lower translucency.<sup>51, 55, 59-62</sup> More importantly, there is statistically significant difference between the HT and LT groups for all thickness groups. Thus, the higher TP observe in the HT group is likely a result of larger crystals of LD as mention in the literature.<sup>8, 47</sup>

The thickness-dependence of TP has been shown in different studies.<sup>51, 55, 59-62</sup> However, this makes the comparison between the materials difficult since many studies used samples of different thicknesses. Also, these studies don't provide an explanation on

the effects of thickness on the change on the TP. In our research team, we applied the general Beer-Lambert law equation on TP as following:

$$TP/TP_0 = e^{-\rho l} \quad (10)$$

TP is the translucency parameter measured at any thickness.

TP<sub>0</sub> is the translucency parameter when the thickness approach 0.

$\rho$  is the coefficient of TP.

$l$  is the thickness of the sample.

After creating a log relationship between the thickness and the TP as shown (Fig 21, 22) we can define the coefficient of TP ( $\rho$ ) from the slope of the curve. Similar to the coefficient of absorption, coefficient of TP represents the rate at which the TP changes as the thickness of the changes. The coefficient of TP is summarized in the (Table XXVIII) .The coefficient of TP for the HT group is statistically lower than the LT group. The result indicates that the HT and LT fired at the recommend temp show statistically significant difference in the rate of the change on the TP between the two groups with a higher rate of change seen in the LT group as the thickness increase. It can also be observed that there is statistically a higher TP in the HT group compare to the LT group at 750 °C and 820 °C, but statistically significant difference between the recommended and the 750°C and 820°C groups. The result indicates that shift in color during the firing has a significant effect on the coefficient of TP.

Another important parameter is the TP<sub>0</sub>. There is significant higher TP<sub>0</sub> of the recommended group compared to 750°C and 820°C showing a higher translucency of the samples as the thickness approaches to 0. This is observed in both HT and LT groups. However, there is no statistically significant difference in TP<sub>0</sub> between the HT and LT at

the recommended temperature (Fig 23, 24). The results of the  $TP_o$  and coefficient of TP are summarized in table (Table XXIX, XXX)

The result indicates that at a very thin thickness, the two materials show the same translucency. However, the smaller crystal sizes in the LT group significantly increase the scattering of light wavelength as the samples thickness increases and show a higher rate of change in reducing the TP of the sample, when compared to the HT group.

#### RESULT ON TP SCE

We preformed 2-way ANOVA statically analysis on TP that calculated from SCE with p value less than 0.05. All Pairwise Multiple Comparison Procedures (Holm-Sidak method) show the overall significance level = 0.05. (Table XXXI, XXXII)

The TP calculated form SCE for the HT group decreases at the recommended temperature from 23.2 to 13.61 as the thickness increases from 1 to 2mm. The TP for the LT group decrease from 19.99 to 10.74 as the thickness increase from 1 to 2mm. There is statistically significant difference between the thickness groups within the HT group and the same observation is seen in the LT group (Table XXXIII, XXXIV). The result is expected since the higher material thickness absorbs more light and result in lower translucency. More importantly, there is statistically significant difference between the HT and LT groups in all thickness groups (Fig 25). In general, SCE is slightly higher than SCI in all thickness groups. This indicates the fact that the surface roughness increases the TP.<sup>61</sup> Moreover, the above equation was applied to SCE as well and a similar trend was observed (Fig 26-29) (Table XXXV-XXXVII).

Many authors have tried to correlate CR and TP<sup>47, 58</sup> as well as CR ratio and transmittance percentage.<sup>59</sup> Barizon et al.<sup>58</sup> and Della Bona et al.<sup>47</sup> found linear relationship between CR and TP. However, Spink et al.,<sup>59</sup> pointed out that the linear relationship breaks down when the CR is high and translucency approaches 50%.

We first plotted the data of the mean irradiance and TP for the recommended temperature group and the plot shows that there is a linear relationship between TP and mean irradiance (Fig 30). Both HT and LT groups also follow the linear relationship. Thus, it can be seen that the translucency of the materials is directly correlated to the mean irradiance passing through the samples. The result shows that when the HT and LT groups have the same TP, they allow the same mean irradiance that comes out from the bottom surface the samples (Fig 31).

Moreover, when we plotted our data from all groups comparing TP and T% as well as TP and CR, we found that there is a linear relationship between TP and T% and also between TP and CR. Moreover, when comparing the HT and LT groups that have the same TP, the LT group has a higher contrast ratio (Fig 32-35).

## FIGURES AND TABLES

FIGURE 1. Diamond saw (Isomet 1000, Buehler, Lake Forest, IL).

FIGURE 2. Ivoclar Vivadent ceramic furnace  
(Programat® CS).

FIGURE 3. Samples were ready for firing.



FIGURE 4. Samples after three firing temperatures. They arranged from the left to the right according to the firing temperature (750, 840, and recommended receptively). The top samples belong to the HT group and below to them are the LT group.

FIGURE 5. Diagram of the study design.

FIGURE 6. Spectrophotometer (CM-2600D).

FIGURE 7. Example of samples on white and black background. The samples should be placed separately in each background before using the spectrophotometer.

FIGURE 8. Managing Accurate Resin Curing (MARC®), resin calibrator.

FIGURE 9. A sample placed between the bottom sensor of the resin calibrator and the curing light tip.

FIGURE 10. The top sensor of the resin calibrator measuring the mean irradiance of the curing unit light.

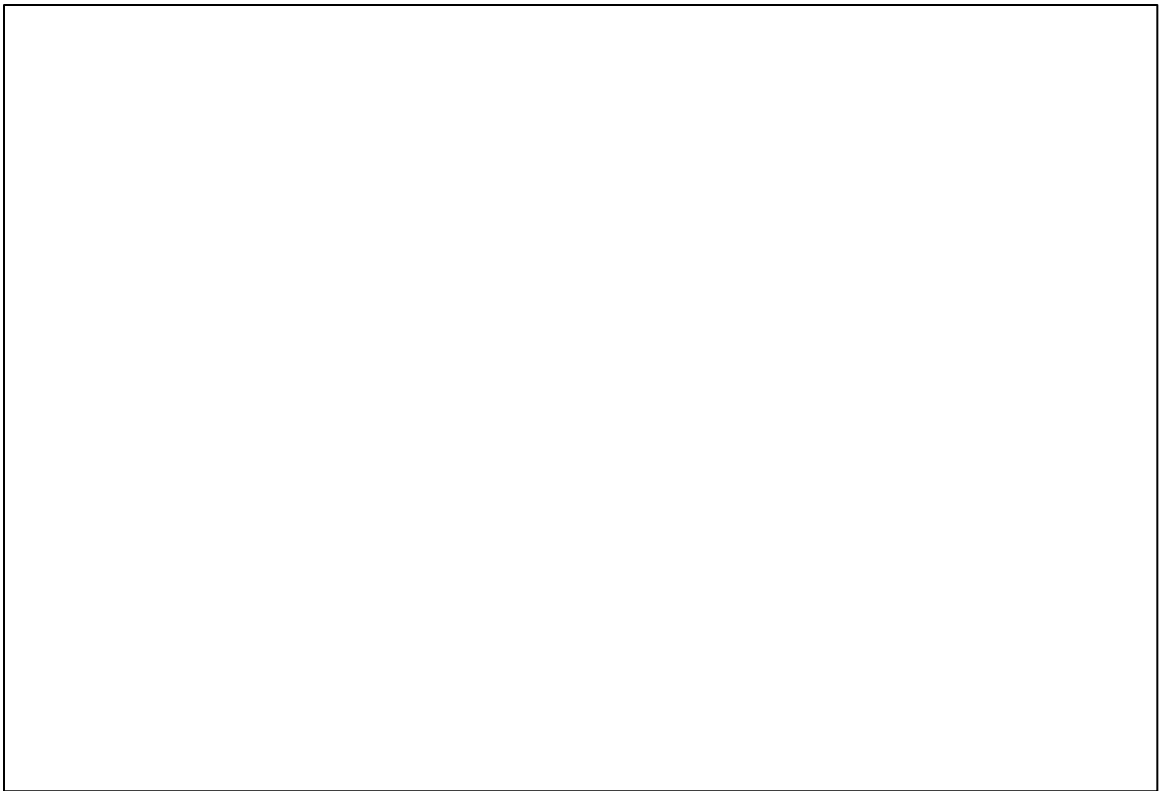


FIGURE 11. Mean irradiances of the recommended group for all thicknesses.



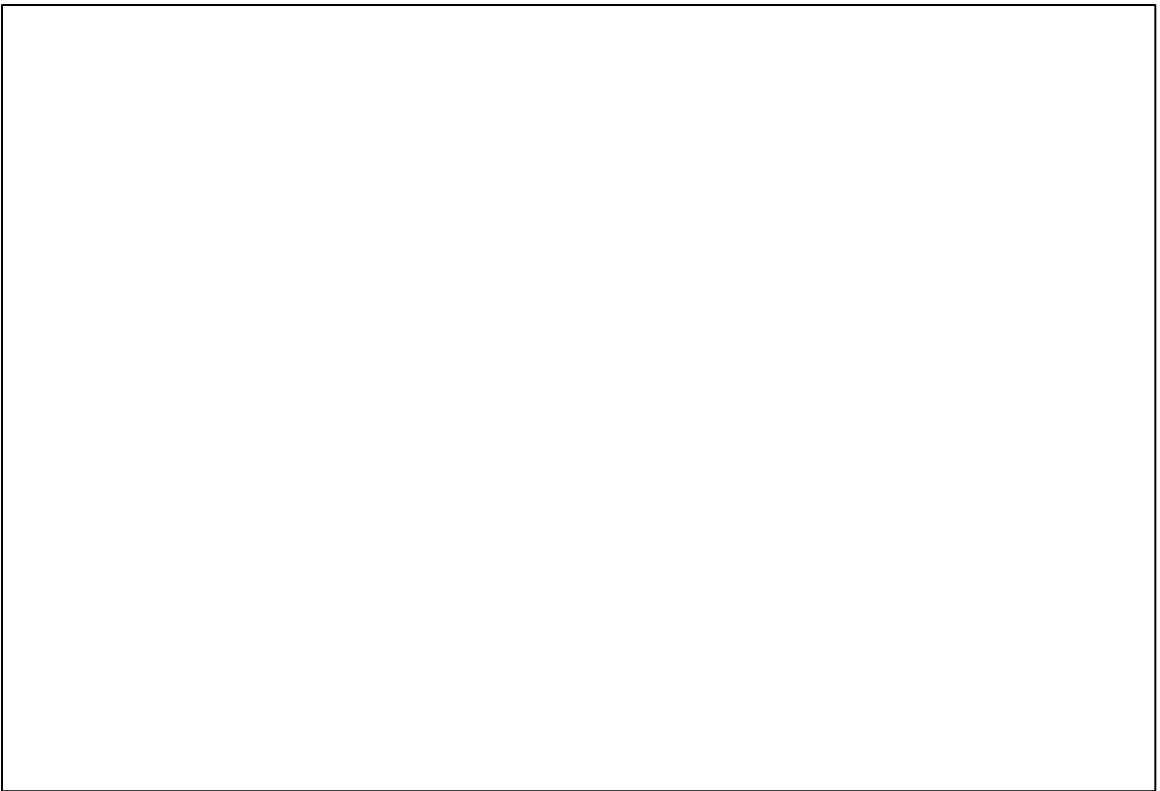


FIGURE 12. A logarithmic plot of the mean irradiance in each thickness for the HT group.

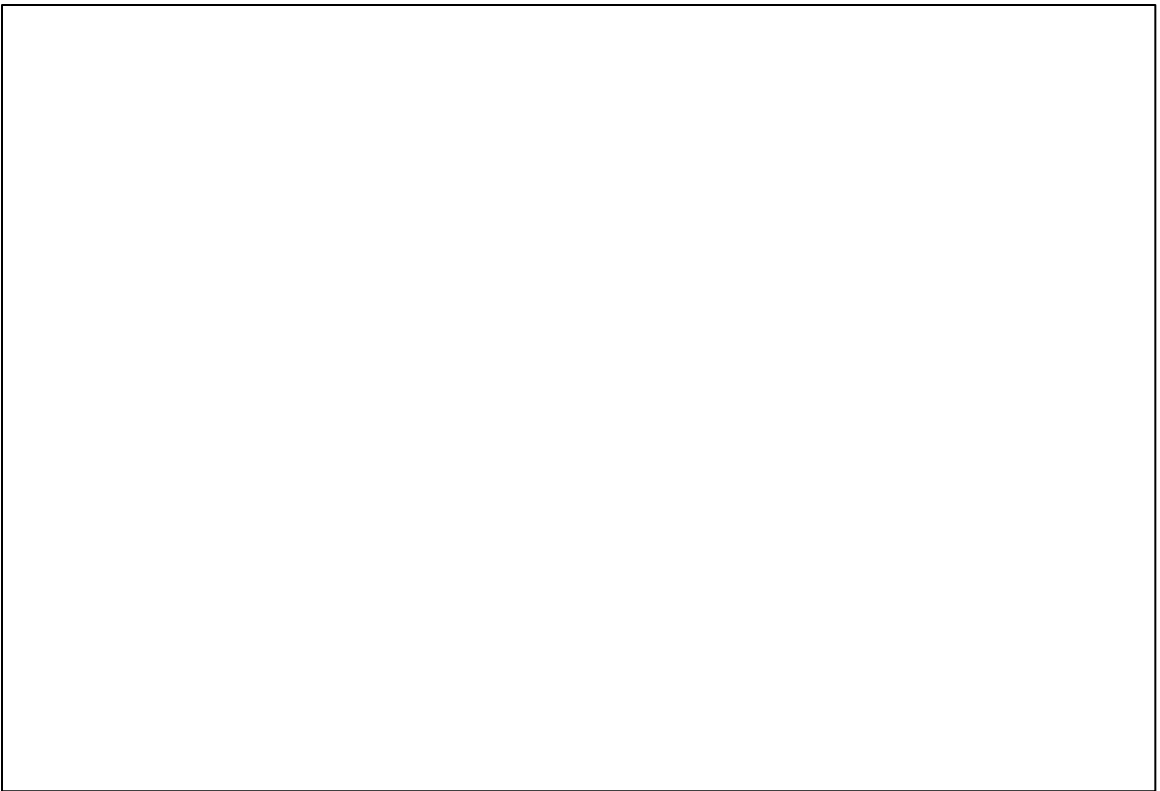


FIGURE 13. A logarithmic plot of the mean irradiance in each thickness for the LT group.

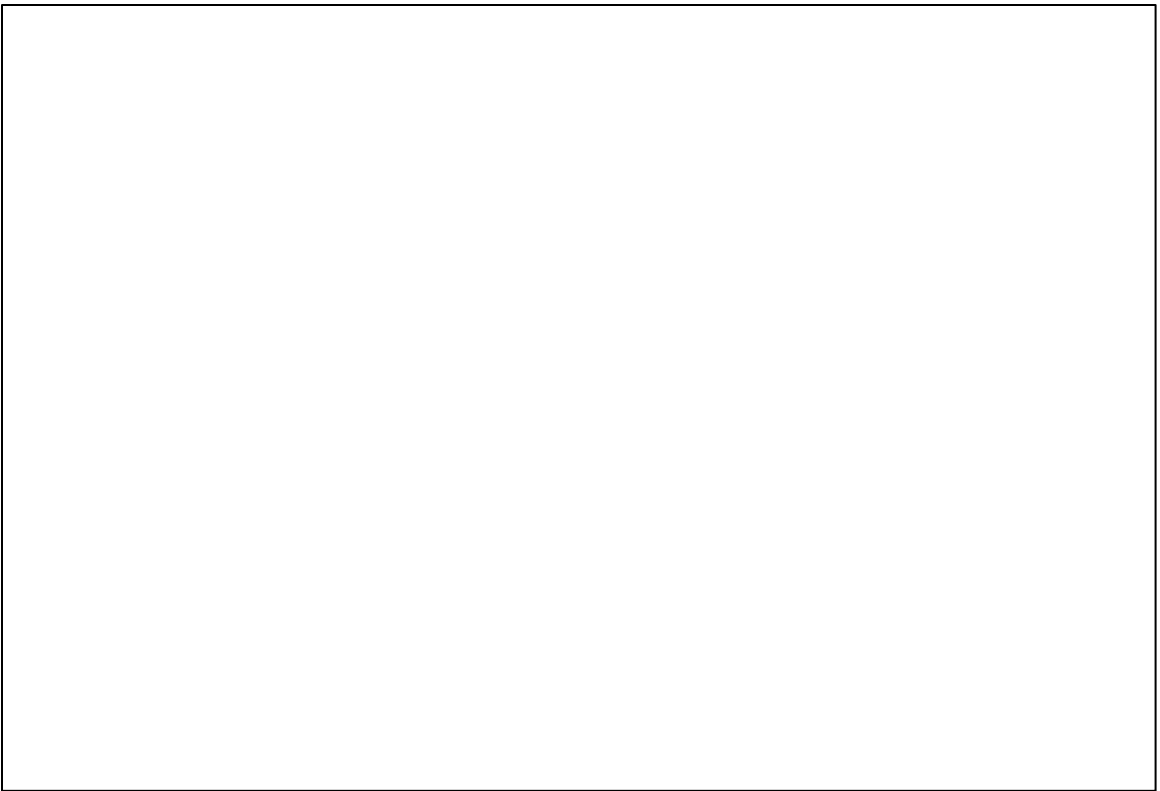


FIGURE 14. Effective incident irradiances for both HT and LT groups in different firing temperatures.

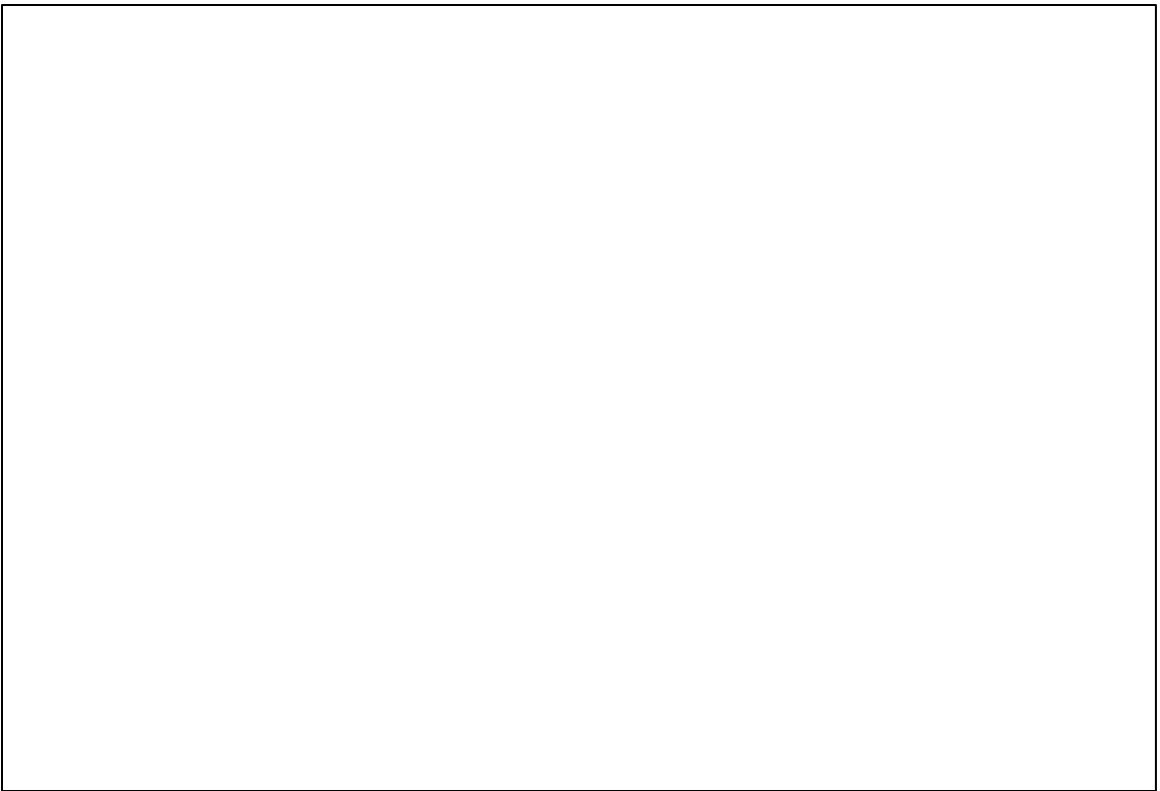


FIGURE 15. Spectral peaks of the HT group in each thickness for the different firing temperatures.

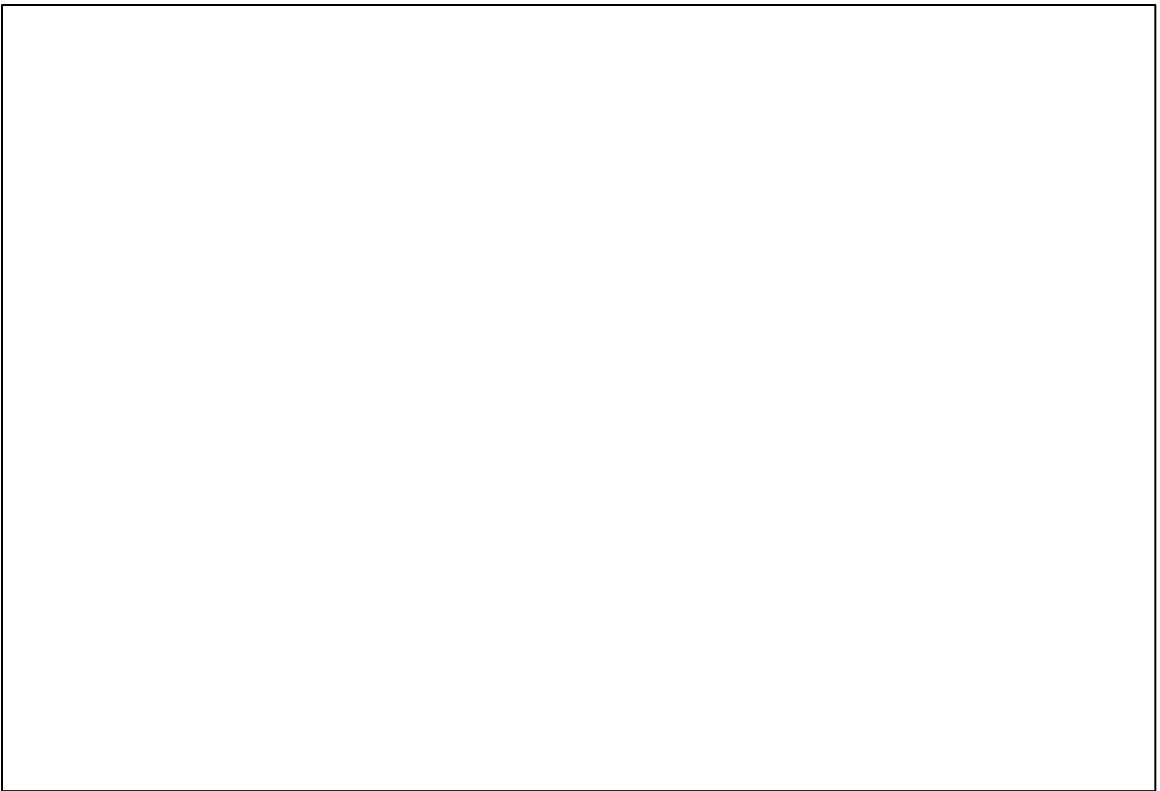


FIGURE 16. Spectral peaks of the LT group in each thickness for the different firing temperatures.

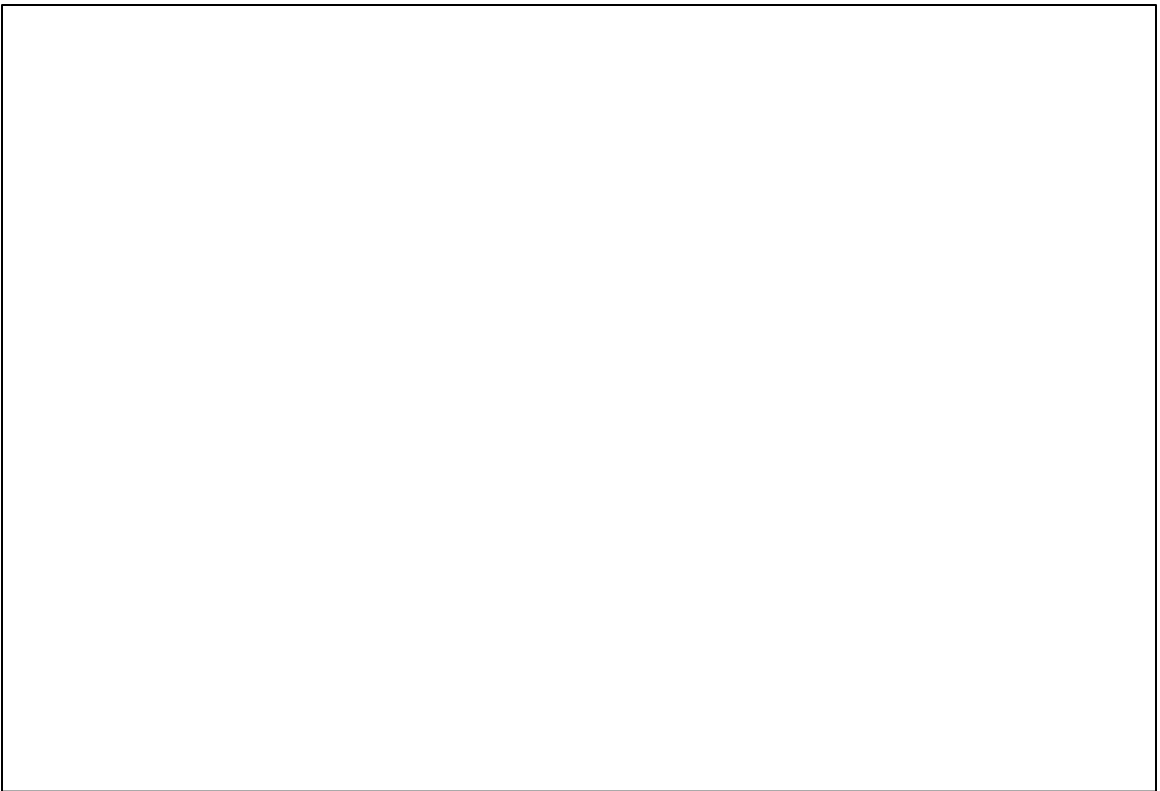


FIGURE 17. Mean CIE L\* value for both HT and LT groups in different firing temperatures.

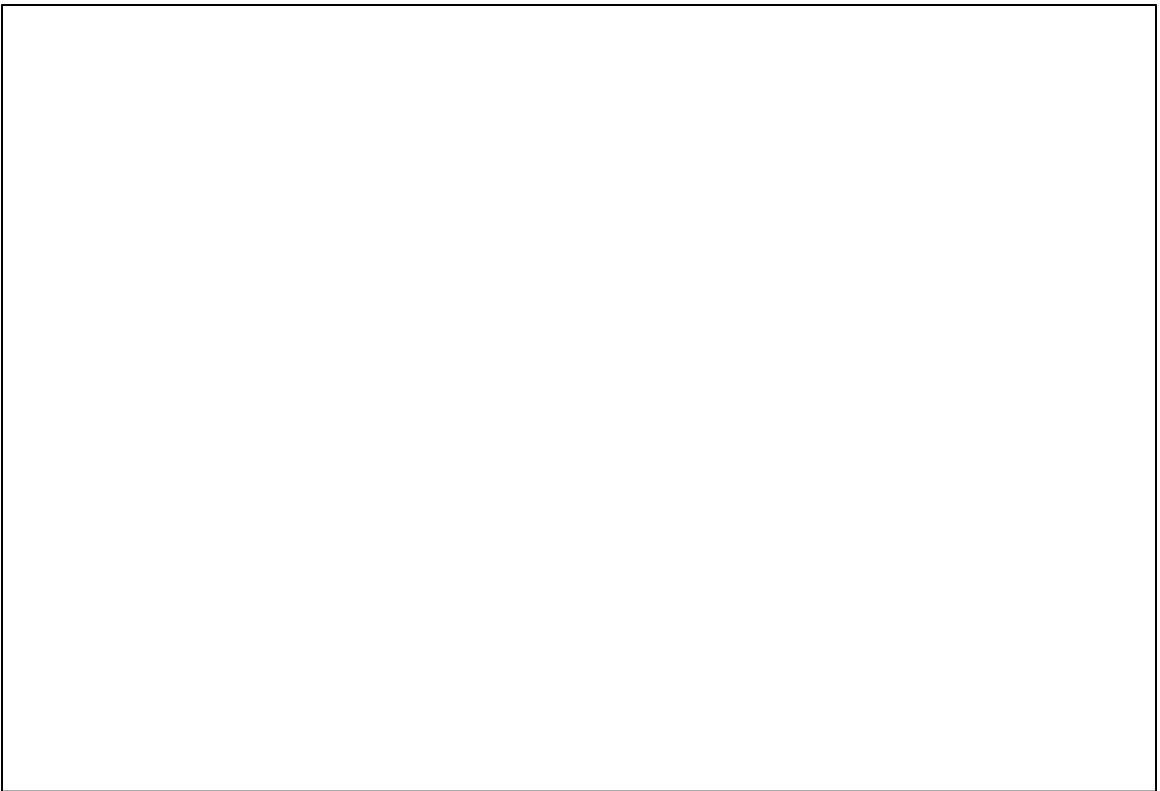


FIGURE 18. Mean CIE  $a^*$  value for both HT and LT groups in different firing temperatures.

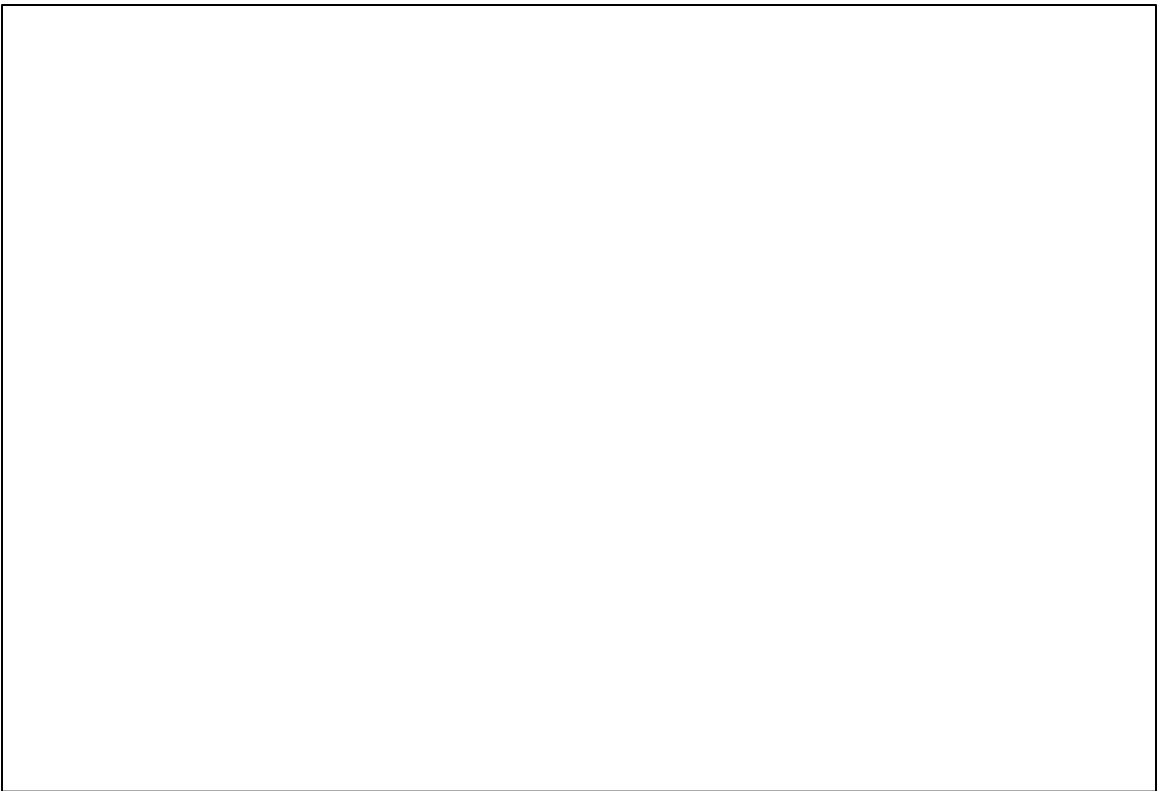


FIGURE 19. Mean CIE  $b^*$  value for both HT and LT groups in different firing temperatures.



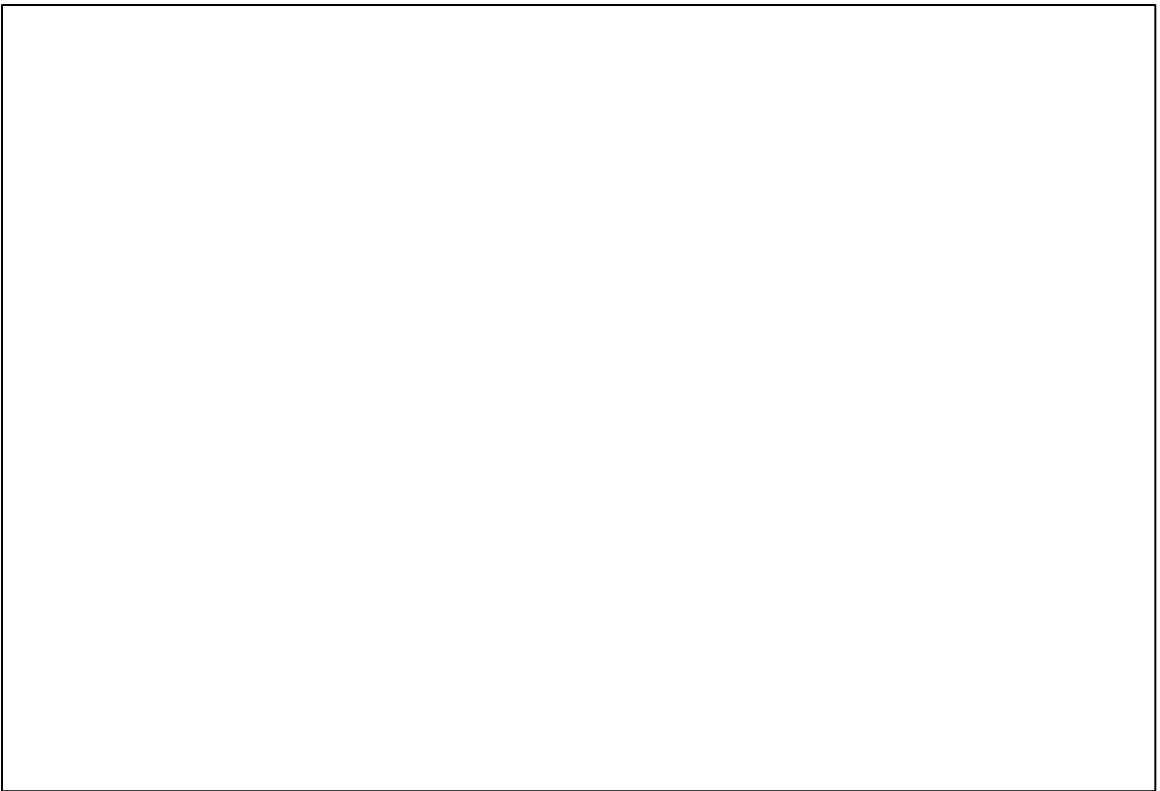


FIGURE 20. Translucency parameter measured from SCI in each thickness of the recommended temperature for both HT and LT groups.

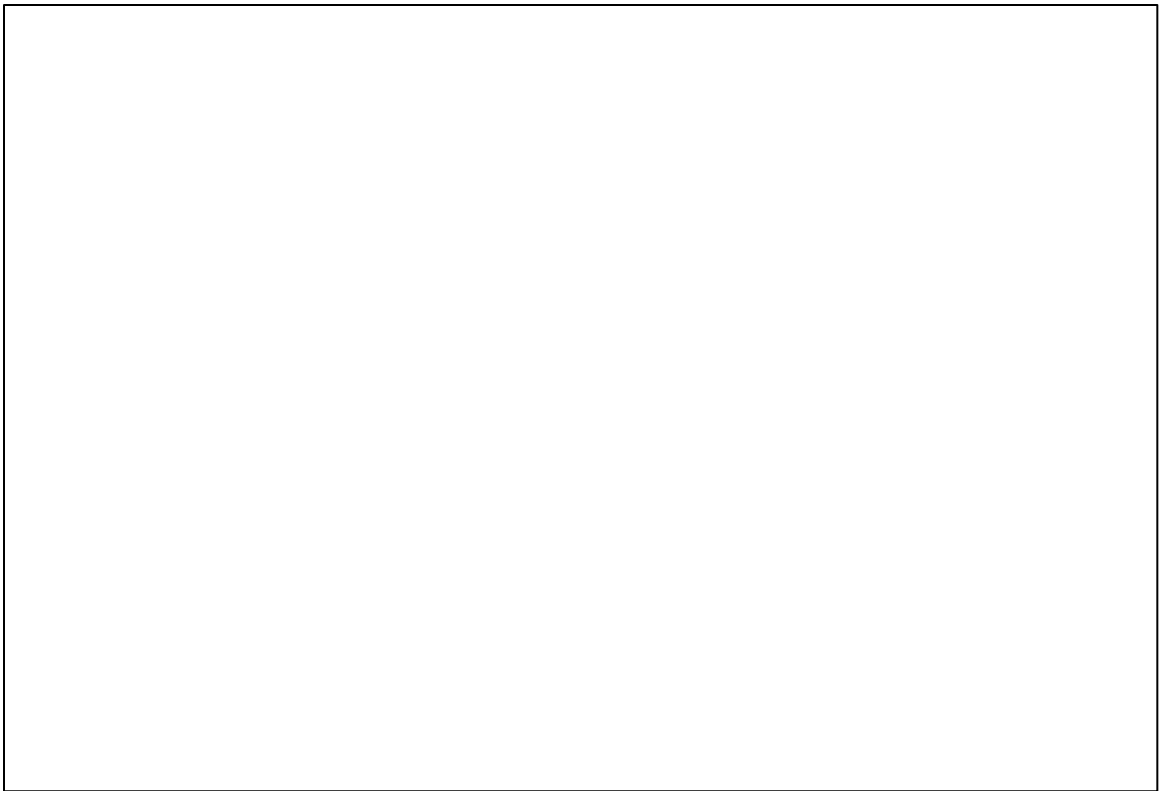


FIGURE 21. A logarithmic plot of the translucency parameter measured from SCI in each thickness for the HT group.

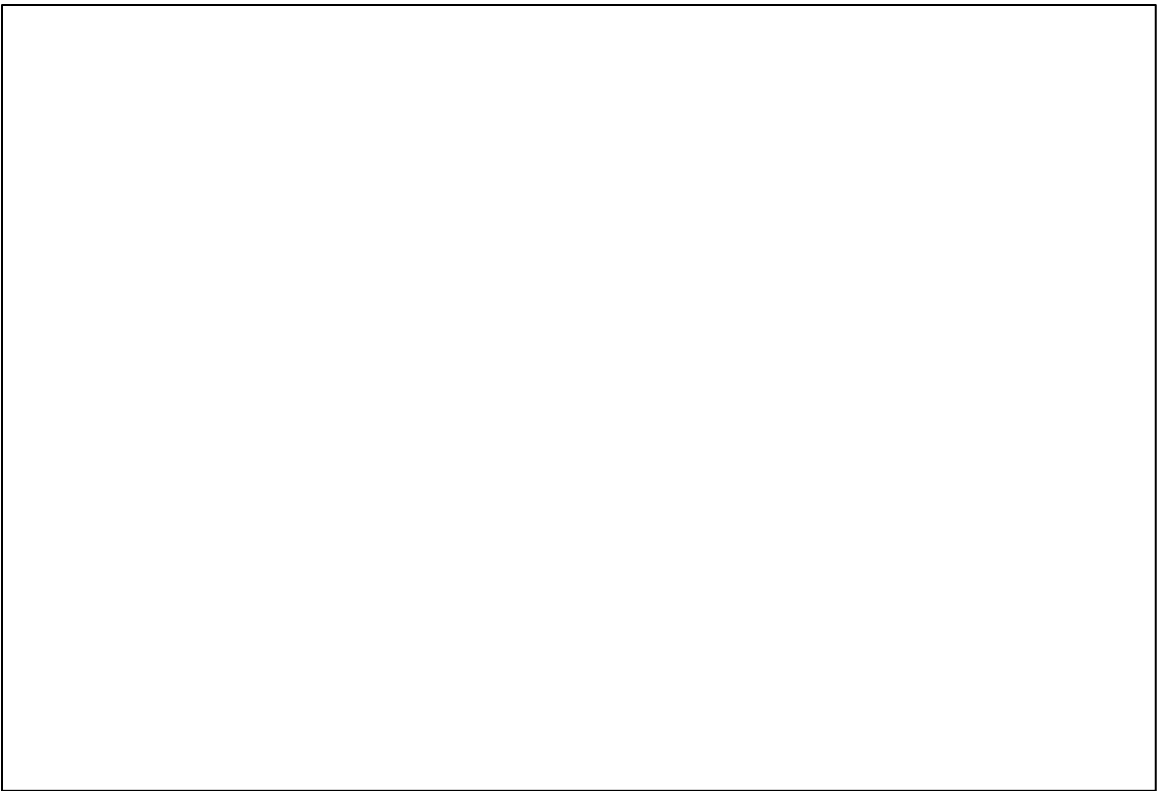


FIGURE 22. A logarithmic plot of the translucency parameter measured from SCI in each thickness for the LT group.

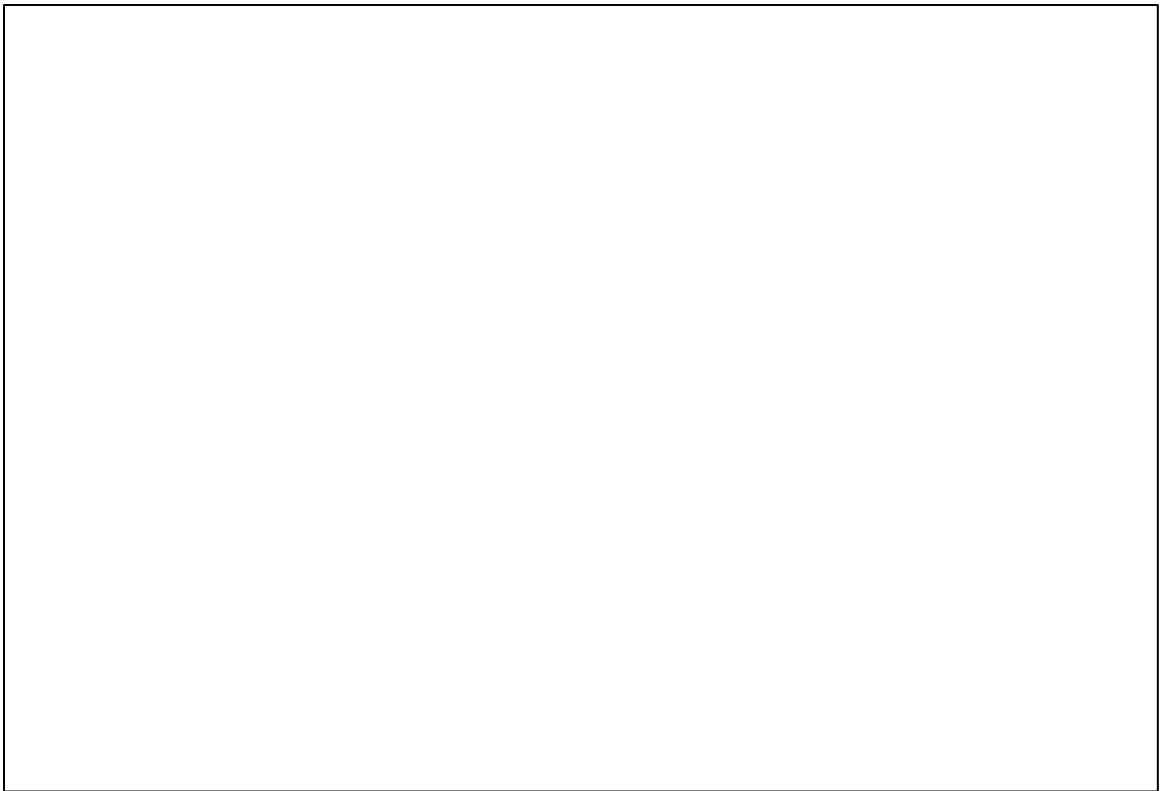


FIGURE 23. Relation of translucency parameter measured from SCI in each thickness of the recommended temperature for both HT and LT groups.

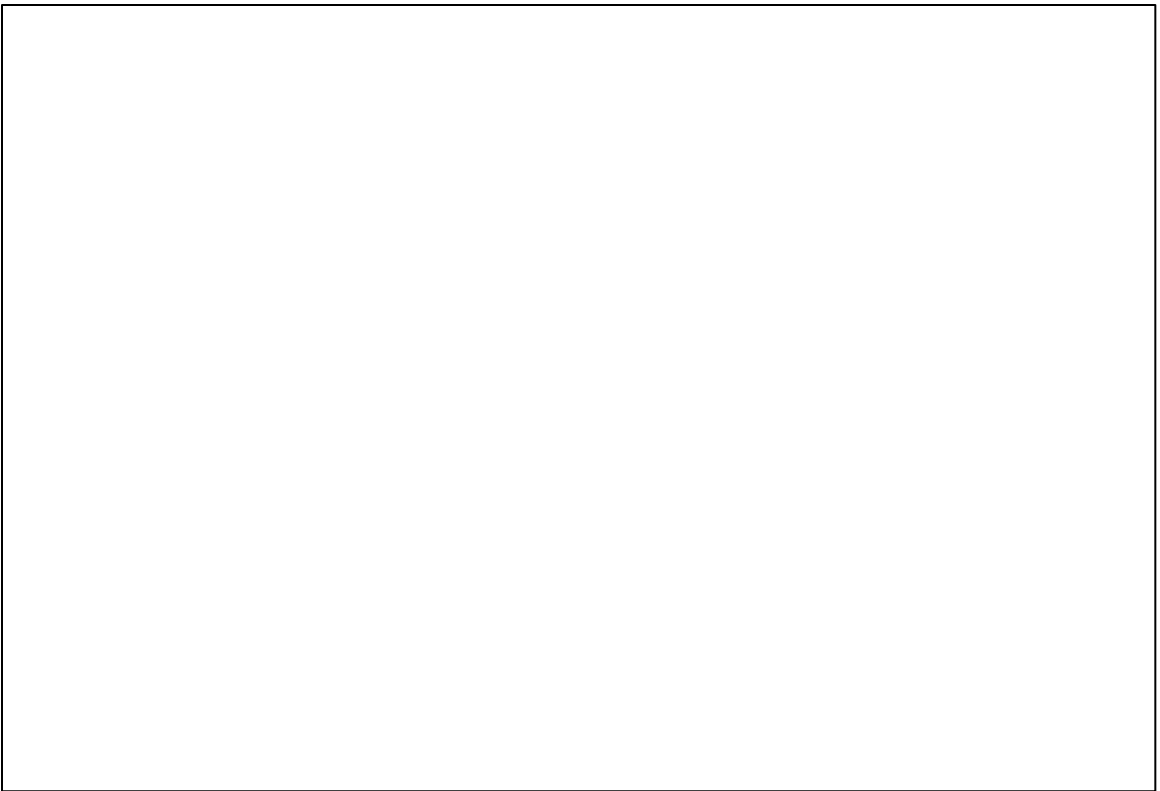


FIGURE 24.  $TP_0$  measured SCI for both HT and LT groups for each firing temperature.

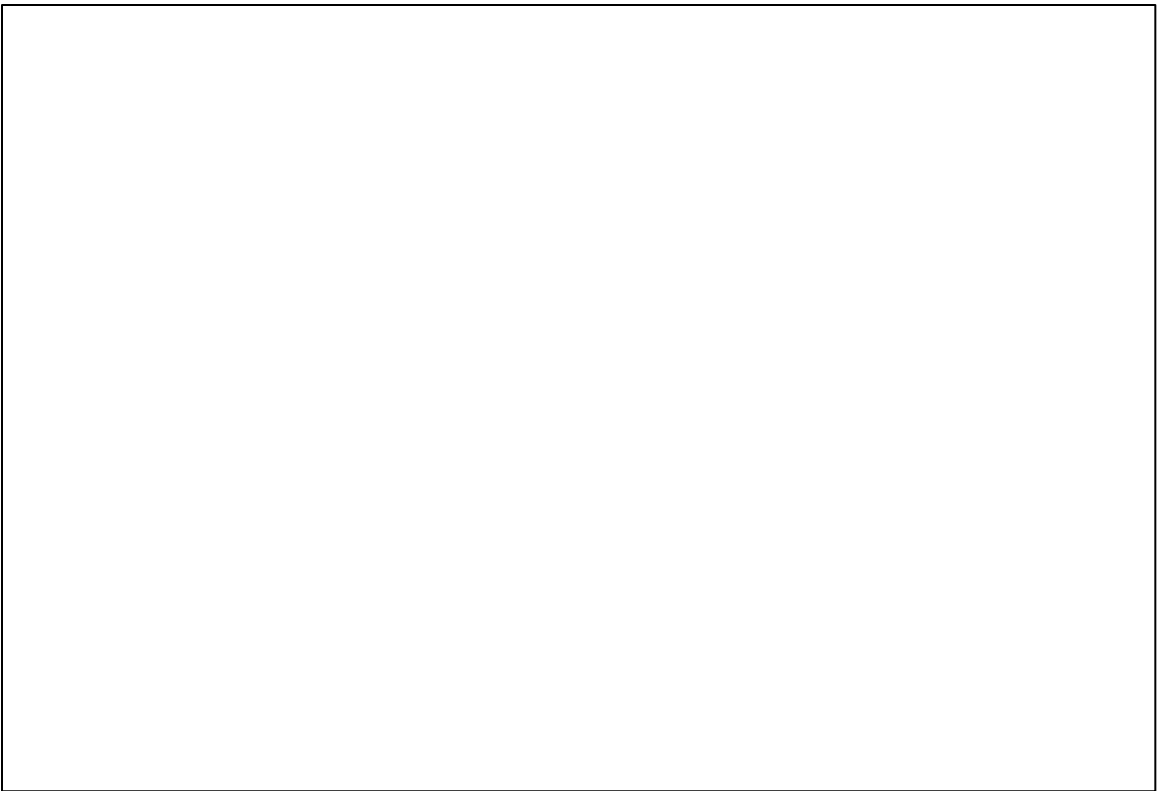


FIGURE 25. Translucency parameter measured from SCE in each thickness of the recommended temperature for both HT and LT groups.

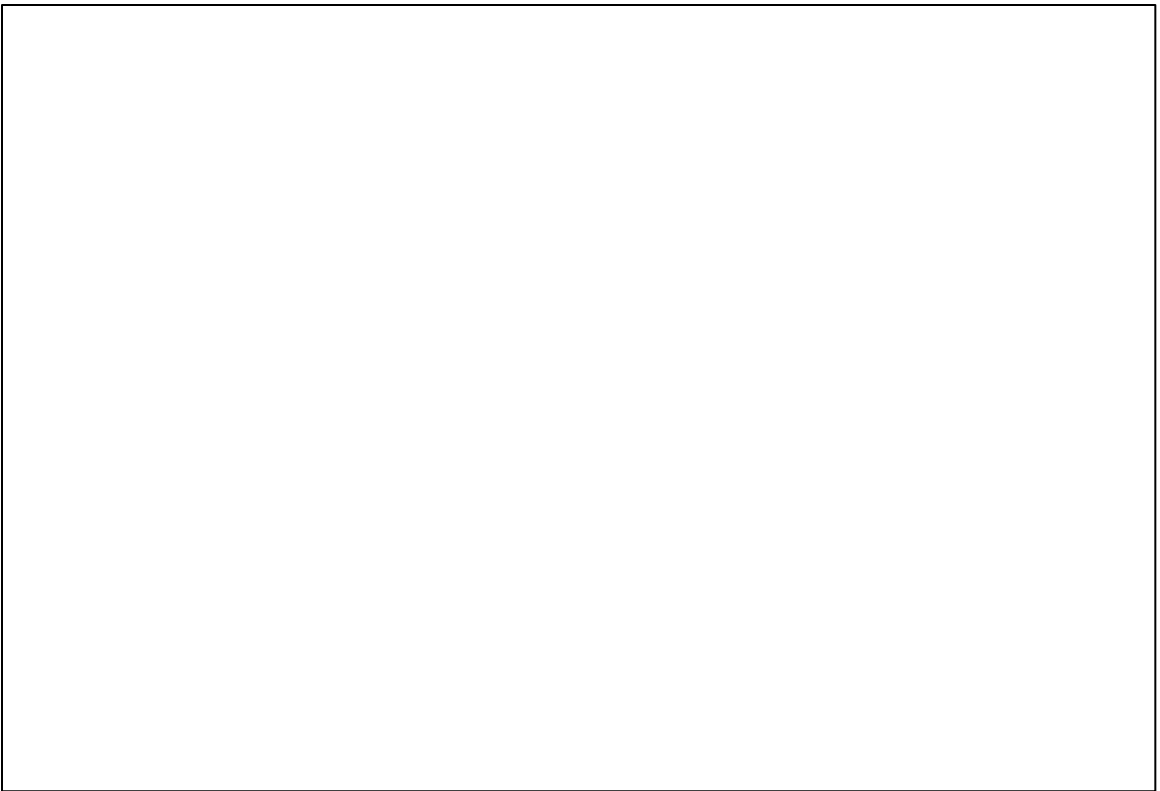


FIGURE 26. Logarithmic plot of the translucency parameter measured from SCE in each thickness for the HT group.

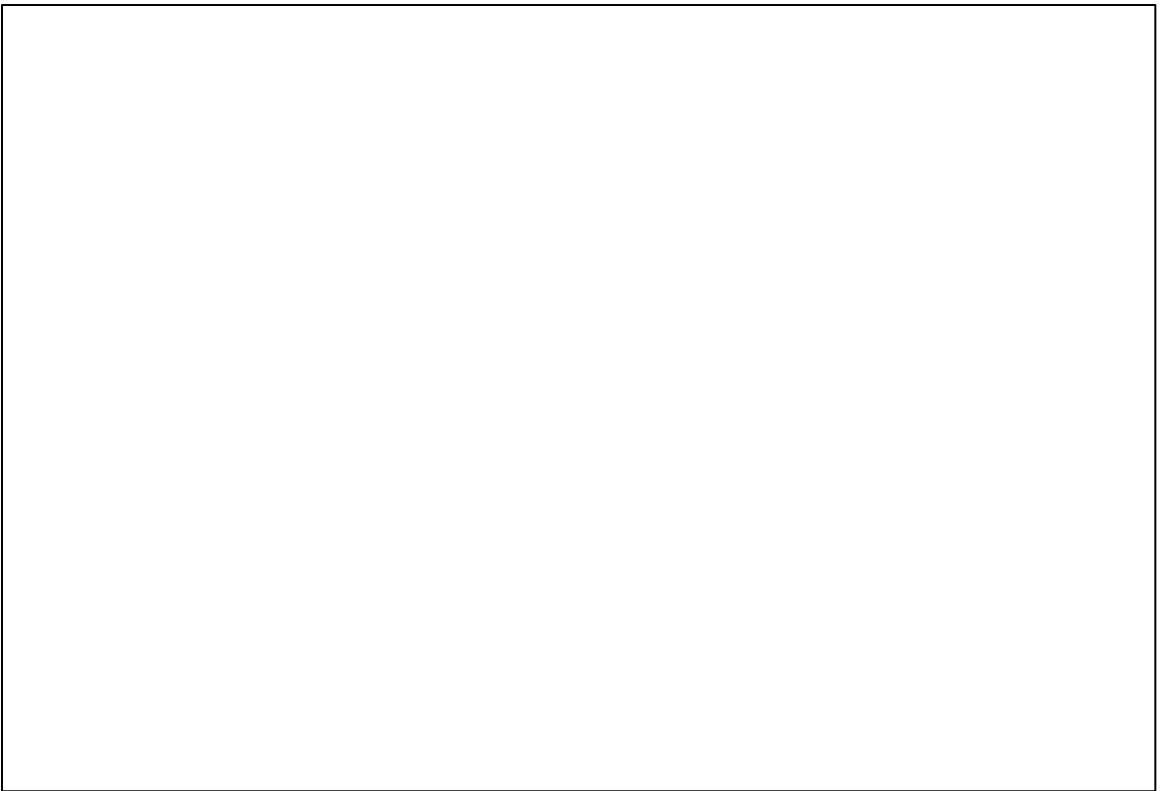


FIGURE 27. Logarithmic plot of the translucency parameter measured from SCE in each thickness for the LT group.



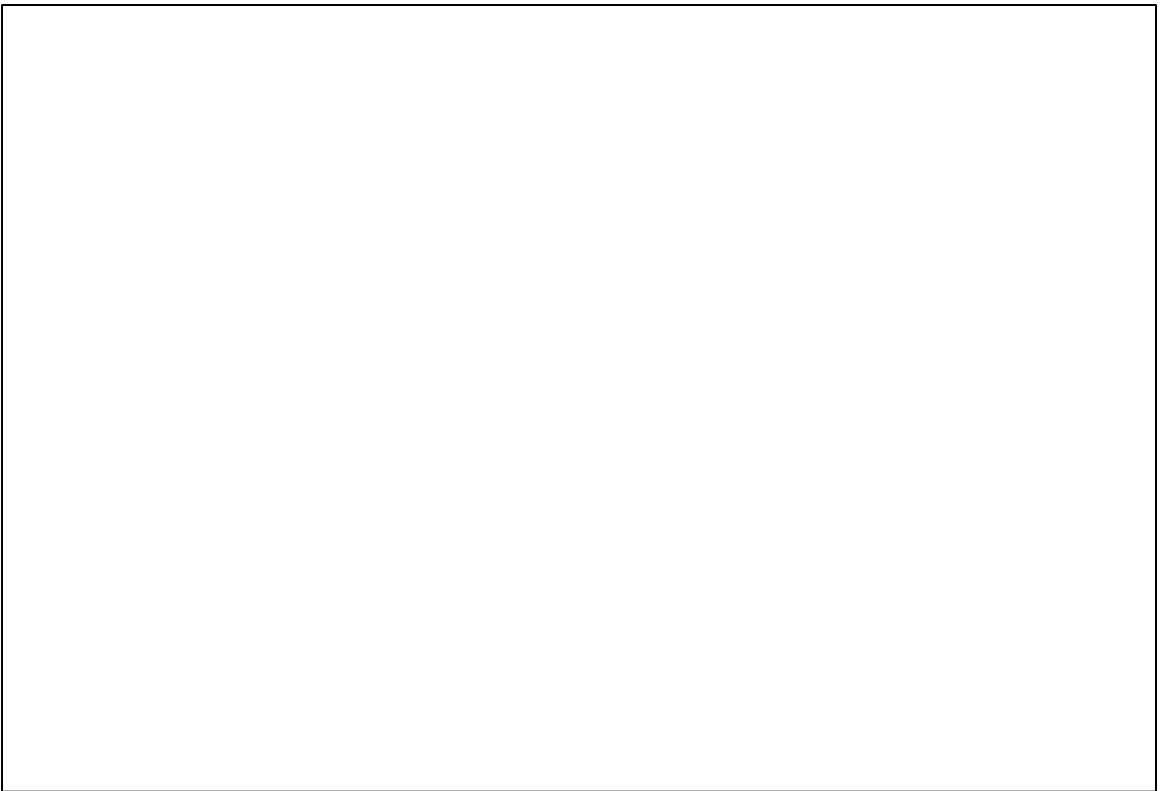


FIGURE 28. Relation of translucency parameter measured from SCE in each thickness of the recommended temperature for both HT and LT groups.

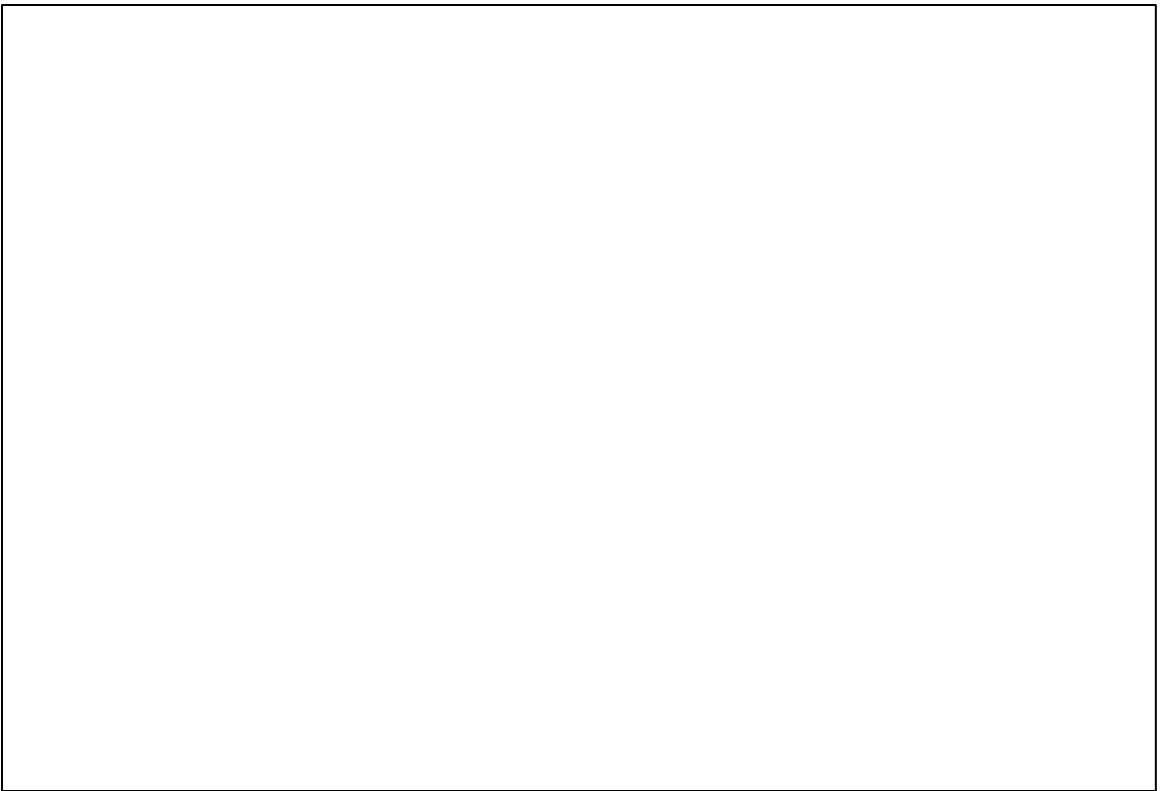


FIGURE 29.  $TP_0$  measured from SCE for both HT and LT groups for each firing temperature.



FIGURE 30. Correlation between the translucency parameter and mean irradiance of both HT and LT groups for the recommended temperatures.



FIGURE 31. Correlation between translucency parameter and mean irradiance for all groups.

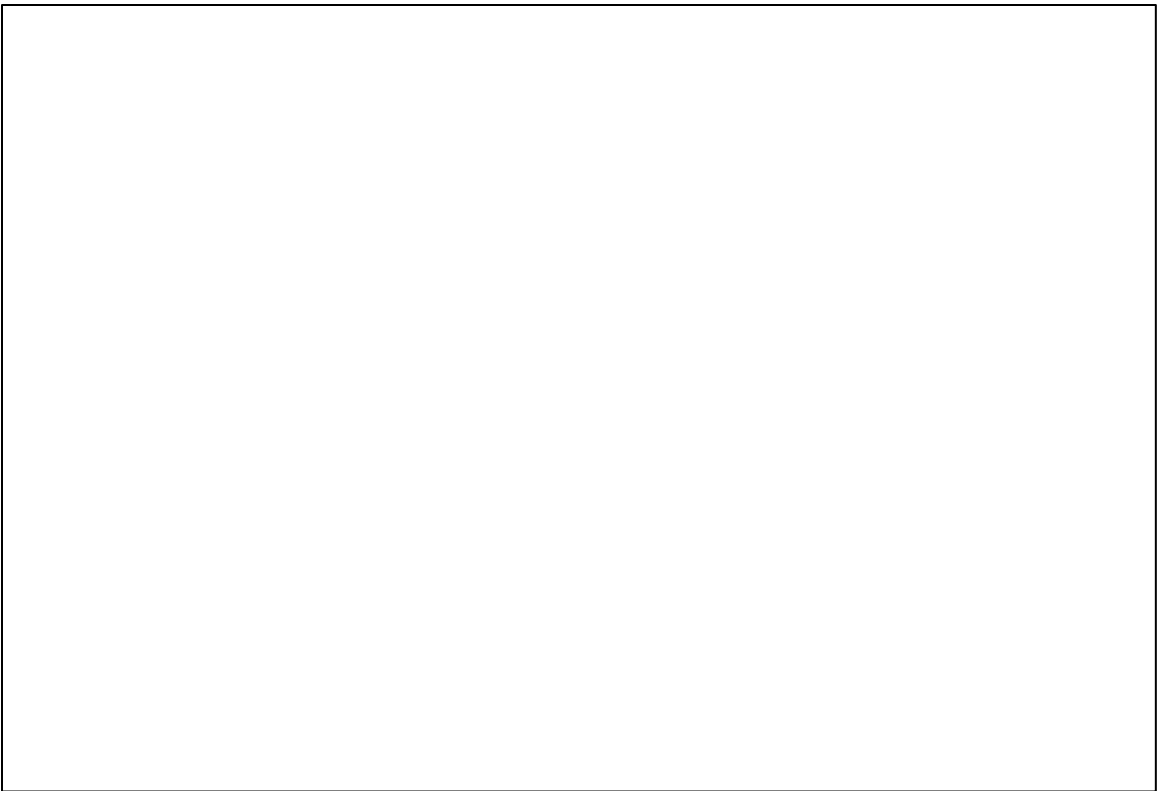


FIGURE 32. Correlation between the translucency parameter and contrast ratio measured from SCI of both HT and LT groups for the recommended temperatures.

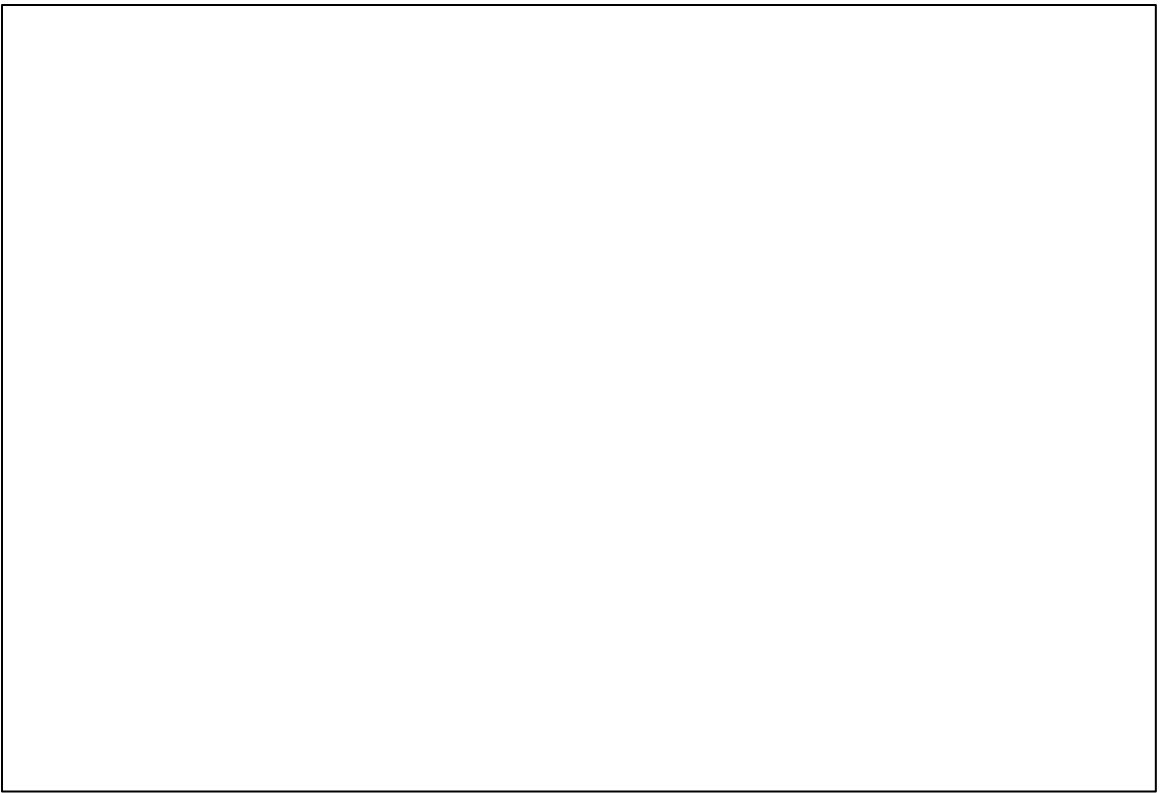


FIGURE 33. Correlation between the translucency parameter and contrast ratio measured from SCE of both HT and LT groups for the recommended temperatures.

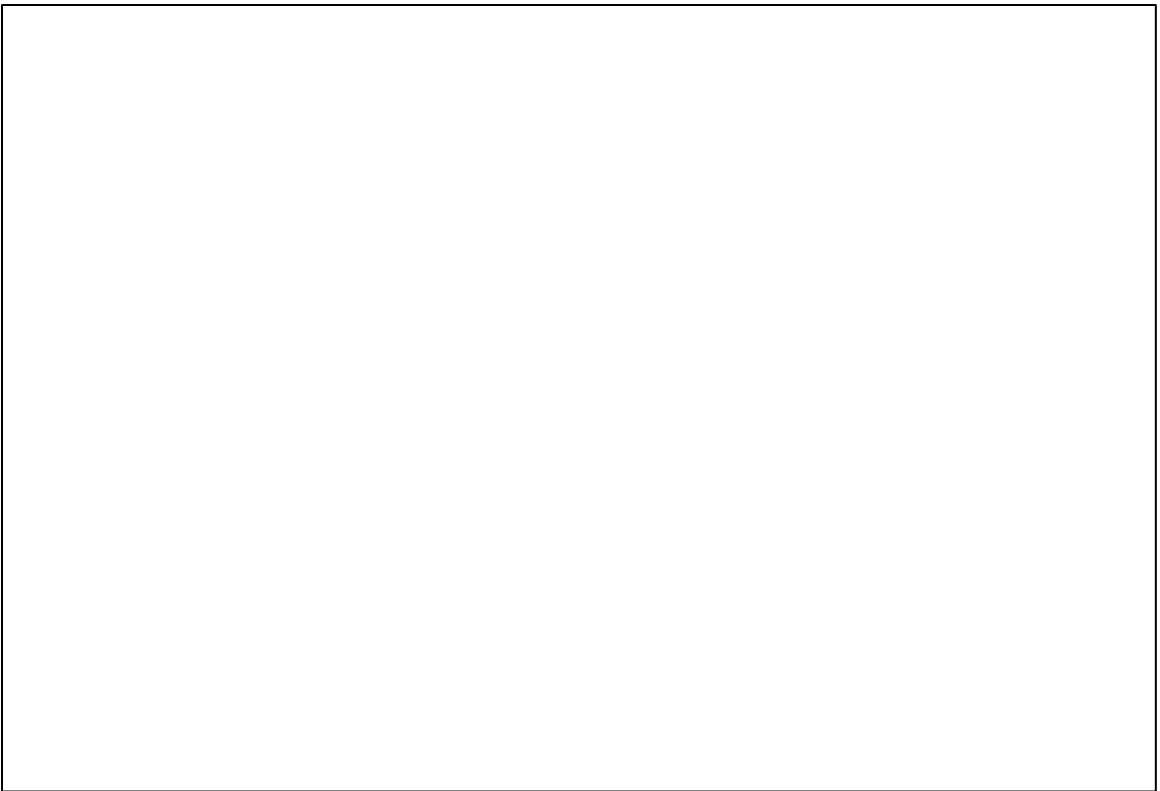


FIGURE 34. Correlation between the transmission percentage and contrast ratio measure from SCI of both HT and LT groups for the recommended temperatures.

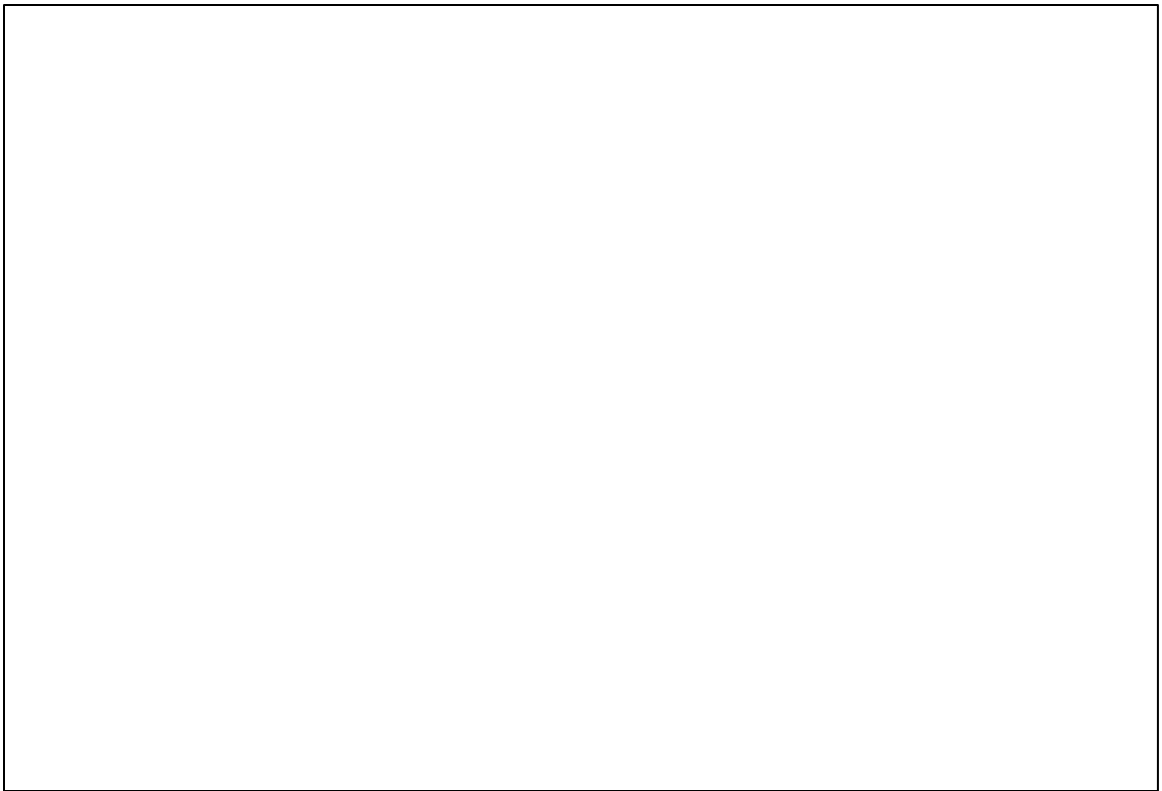


FIGURE 35. Correlation between the transmission percentage and contrast ratio measure from SCE of both HT and LT groups for the recommended temperatures.



TABLE I  
Phase formation sequences in the lithium disilicate glass-ceramic

Temperature range (°C)	Reaction sequence
500–580	Induction period of nucleation
580–620	Nucleation of $\text{Li}_2\text{SiO}_3$ and $\text{Li}_2\text{Si}_2\text{O}_5$
620–730	Nuclei of both $\text{Li}_2\text{SiO}_3$ and $\text{Li}_2\text{Si}_2\text{O}_5$ saturated; formation
740–780	$\text{Li}_2\text{SiO}_3$ to $\text{Li}_2\text{Si}_2\text{O}_5$ transformation
780–860	Crystal growth of $\text{Li}_2\text{Si}_2\text{O}_5$ ; formation of $\text{Li}_3\text{PO}_4$ crystals the precipitation of $\text{ZrO}_2$
860–950	Melting of $\text{Li}_2\text{Si}_2\text{O}_5$ and $\text{ZrO}_2$
950–1010	Melting of $\text{Li}_3\text{PO}_4$

TABLE II  
The heating schedule of the three different firing temperatures

TABLE III  
The mean, standard deviation, standard error, minimum and maximum for the mean irradiance ( $\text{mW}/\text{cm}^2$ )

Translucency	Firing Temp	Thickness	N	Mean	SD	Minimum	Maximum
HT	750	1	4	164.72	4.35	158.66	168.86
		1.25	4	130.44	11.04	119.41	140.89
		1.5	4	91.59	7.18	85.35	98.06
		1.75	4	70.20	6.23	63.50	77.80
		2	4	47.54	1.03	46.64	48.70
	820	1	4	142.56	5.61	135.51	148.70
		1.25	4	98.70	12.92	86.08	116.65
		1.5	4	64.99	2.43	62.21	68.03
		1.75	4	49.82	5.34	45.10	56.97
		2	4	33.17	1.53	31.59	35.13
	Rec	1	4	331.78	6.42	325.22	338.22
		1.25	4	297.39	7.63	289.24	306.29
		1.5	4	256.04	7.72	245.44	263.97
		1.75	4	214.80	2.60	213.04	218.59
		2	4	188.00	3.01	185.14	190.83
LT	750	1	4	170.17	25.34	151.28	205.26
		1.25	4	129.66	5.67	123.95	134.62
		1.5	4	105.46	10.67	90.72	114.66
		1.75	4	68.69	4.97	64.39	75.13
		2	4	58.76	9.12	49.51	70.59
	820	1	4	160.75	20.16	134.36	179.02
		1.25	4	104.96	4.76	99.00	110.63
		1.5	4	70.59	3.34	66.70	73.63
		1.75	4	54.70	7.56	48.36	65.66
		2	4	42.54	5.77	34.14	46.47
	Rec	1	4	276.20	3.85	272.69	281.70
		1.25	4	223.51	3.20	220.08	227.76
		1.5	4	185.06	6.35	181.50	194.57
		1.75	4	145.39	3.88	141.06	150.01
		2	4	121.18	4.73	115.35	126.88

TABLE IV

ANOVA results for the maximum for the mean irradiance ( $\text{mW}/\text{cm}^2$ )

<b>Effect</b>	<b>NumDF</b>	<b>DenDF</b>	<b>FValue</b>	<b>ProbF</b>	<b>sig</b>
Translucency	1	90	128.48	<.0001	*
Firing_Temp	2	90	3221.47	<.0001	*
Thickness	4	90	842.34	<.0001	*
Transluce*Firing_Tem	2	90	256.57	<.0001	*
Translucen*Thickness	4	90	2.07	0.0913	
Firing_Tem*Thickness	8	90	10.94	<.0001	*
Transl*Firing*Thickn	8	90	0.73	0.6646	

TABLE V  
Statistical analysis on mean irradiance for the recommended temperature group

<b>Comparisons within Thickness</b>				
<b>Comparison</b>	<b>Diff of Means</b>	<b>t</b>	<b>P</b>	<b>P&lt;0.050</b>
HT vs. LT	67.333	40.410	<0.001	Yes
<b>Comparisons within 1</b>				
<b>Comparison</b>	<b>Diff of Means</b>	<b>t</b>	<b>P</b>	<b>P&lt;0.05</b>
HT vs. LT	55.575	14.916	<0.001	Yes
<b>Comparisons within 1.25</b>				
<b>Comparison</b>	<b>Diff of Means</b>	<b>t</b>	<b>P</b>	<b>P&lt;0.05</b>
HT vs. LT	73.886	19.831	<0.001	Yes
<b>Comparisons within 1.5</b>				
<b>Comparison</b>	<b>Diff of Means</b>	<b>t</b>	<b>P</b>	<b>P&lt;0.05</b>
HT vs. LT	70.978	19.050	<0.001	Yes
<b>Comparisons within 1.75</b>				
<b>Comparison</b>	<b>Diff of Means</b>	<b>t</b>	<b>P</b>	<b>P&lt;0.05</b>
HT vs. LT	69.404	18.628	<0.001	Yes
<b>Comparisons within 2</b>				
<b>Comparison</b>	<b>Diff of Means</b>	<b>t</b>	<b>P</b>	<b>P&lt;0.05</b>
HT vs. LT	66.822	17.935	<0.001	Yes
<b>Comparisons within HT</b>				
<b>Comparison</b>	<b>Diff of Means</b>	<b>t</b>	<b>P</b>	<b>P&lt;0.05</b>
1.000 vs. 2.000	143.777	38.589	<0.001	Yes
1.000 vs. 1.750	116.982	31.397	<0.001	Yes
1.250 vs. 2.000	109.391	29.360	<0.001	Yes
1.250 vs. 1.750	82.596	22.168	<0.001	Yes
1.000 vs. 1.500	75.743	20.329	<0.001	Yes
1.500 vs. 2.000	68.034	18.260	<0.001	Yes
1.250 vs. 1.500	41.357	11.100	<0.001	Yes
1.500 vs. 1.750	41.239	11.068	<0.001	Yes
1.000 vs. 1.250	34.386	9.229	<0.001	Yes
1.750 vs. 2.000	26.795	7.192	<0.001	Yes

TABLE VI  
 Statistical analysis on mean irradiance for the recommended temperature group  
 (continue)

Comparisons within LT				
Comparison	Diff of Means	t	P	P<0.05
1.000 vs. 2.000	155.024	41.608	<0.001	Yes
1.000 vs. 1.750	130.812	35.109	<0.001	Yes
1.250 vs. 2.000	102.327	27.464	<0.001	Yes
1.000 vs. 1.500	91.147	24.463	<0.001	Yes
1.250 vs. 1.750	78.115	20.966	<0.001	Yes
1.500 vs. 2.000	63.878	17.144	<0.001	Yes
1.000 vs. 1.250	52.697	14.144	<0.001	Yes
1.500 vs. 1.750	39.665	10.646	<0.001	Yes
1.250 vs. 1.500	38.450	10.320	<0.001	Yes
1.750 vs. 2.000	24.213	6.499	<0.001	Yes

TABLE VII  
Summery for the coefficients of absorption

Coefficient of Absorption ( <i>c</i> )				
	HT		LT	
	Mean	SD	Mean	SD
750	1.24	0.07	1.13	0.13
820	1.45	0.08	1.33	0.21
RECOM	0.58	0.02	0.87	0.01

TABLE VIII  
Summary for the effective mean irradiances

$I_e$				
	HT		LT	
	Mean	SD	Mean	SD
750	593.13	57.64	542.08	111.66
820	599.09	80.90	572.81	161.57
RECOM	601.73	21.42	664.29	2.04



TABLE IX  
Statistical analysis on the coefficient of absorption

<b>Comparisons within 750</b>				
<b>Comparison</b>	<b>Diff of Means</b>	<b>t</b>	<b>P</b>	<b>P&lt;0.05</b>
HT vs. LT	0.108	1.397	0.179	No
<b>Comparisons within 820</b>				
<b>Comparison</b>	<b>Diff of Means</b>	<b>t</b>	<b>P</b>	<b>P&lt;0.05</b>
HT vs. LT	0.125	1.616	0.123	No
<b>Comparisons within RECOM</b>				
<b>Comparison</b>	<b>Diff of Means</b>	<b>t</b>	<b>P</b>	<b>P&lt;0.05</b>
LT vs. HT	0.285	3.675	0.002	Yes
<b>Comparisons within HT</b>				
<b>Comparison</b>	<b>Diff of Means</b>	<b>t</b>	<b>P</b>	<b>P&lt;0.05</b>
820.000 vs. RECOM	0.869	11.208	<0.001	Yes
750.000 vs. RECOM	0.654	8.443	<0.001	Yes
820.000 vs. 750.000	0.214	2.765	0.013	Yes
<b>Comparisons within LT</b>				
<b>Comparison</b>	<b>Diff of Means</b>	<b>t</b>	<b>P</b>	<b>P&lt;0.05</b>
820.000 vs. RECOM	0.459	5.917	<0.001	Yes
750.000 vs. RECOM	0.261	3.371	0.007	Yes
820.000 vs. 750.000	0.197	2.545	0.020	Yes

TABLE X  
The mean, standard deviation, standard error, minimum and maximum for the spectral peak (nm)

Translucency	Firing Temp.	Thickness	N	Mean	SD	Minimum	Maximum
HT	750	1	4	458.63	3.64	454.71	462.41
		1.25	4	461.86	1.32	460.83	463.79
		1.5	4	433.70	22.21	419.42	466.49
		1.75	4	405.00	18.32	390.45	431.73
		2	4	377.22	15.60	362.07	392.70
	820	1	4	465.64	2.82	462.00	468.01
		1.25	4	441.50	33.35	401.28	474.13
		1.5	4	380.27	17.88	363.42	397.62
		1.75	4	363.89	0.73	363.21	364.92
		2	4	364.40	3.33	362.00	369.33
	Rec	1	4	485.88	2.59	482.45	488.42
		1.25	4	483.39	3.49	479.01	486.78
		1.5	4	487.39	3.26	483.40	491.16
		1.75	4	485.99	1.05	485.20	487.53
		2	4	484.65	5.57	478.65	491.98
LT	750	1	4	465.50	1.26	464.14	467.17
		1.25	4	464.69	3.40	460.34	468.42
		1.5	4	448.17	17.90	432.03	466.21
		1.75	4	421.27	27.53	397.80	455.98
		2	4	379.13	30.85	363.14	425.39
	820	1	4	466.83	2.41	463.31	468.56
		1.25	4	452.89	17.68	428.00	468.49
		1.5	4	410.12	41.77	368.76	468.22
		1.75	4	371.35	16.12	361.43	395.42
		2	4	372.13	15.58	362.14	395.32
	Rec	1	4	486.77	1.98	483.96	488.29
		1.25	4	488.27	1.38	486.64	489.52
		1.5	4	488.14	2.07	485.06	489.45
		1.75	4	490.01	1.22	488.69	491.57
		2	4	490.58	0.89	489.86	491.77

TABLE XI  
ANOVA results for the spectral peak

<b>Effect</b>	<b>NumDF</b>	<b>DenDF</b>	<b>FValue</b>	<b>ProbF</b>	<b>sig</b>
Translucency	1	90	7.51	0.0074	*
Firing_Temp	2	90	269.13	<.0001	*
Thickness	4	90	67.91	<.0001	*
Transluce*Firing_Tem	2	90	0.72	0.4901	
Translucen*Thickness	4	90	0.54	0.7080	
Firing_Tem*Thickness	8	90	22.19	<.0001	*
Transl*Firing*Thickn	8	90	0.43	0.9024	

TABLE XII  
The mean, standard deviation, standard error, minimum and maximum for CIEL\*  
measured from SCI

Analysis Variable: SCI L*							
Translucency	Firing Temp.	Thickness	N	Mean	SD	Minimum	Maximum
HT	750	1	4	79.50	0.43	78.98	79.96
		1.25	4	77.88	0.98	77.04	79.25
		1.5	4	77.43	0.59	77.04	78.29
		1.75	4	77.52	0.30	77.25	77.93
		2	4	77.74	0.51	77.07	78.18
	820	1	4	82.85	0.89	81.75	83.68
		1.25	4	82.51	0.41	82.12	82.89
		1.5	4	81.24	1.17	79.49	81.93
		1.75	4	81.66	0.42	81.16	82.11
		2	4	81.52	0.12	81.39	81.67
	Rec	1	4	79.94	0.11	79.79	80.04
		1.25	4	76.81	0.42	76.27	77.27
		1.5	4	73.87	0.13	73.72	74.03
		1.75	4	71.17	0.23	70.98	71.50
		2	4	69.14	0.26	68.88	69.48
LT	750	1	4	72.87	1.23	71.14	73.88
		1.25	4	72.06	1.30	70.27	73.38
		1.5	4	71.81	1.33	70.09	72.91
		1.75	4	71.63	1.40	70.29	72.86
		2	4	70.31	1.66	69.40	72.80
	820	1	4	76.09	0.38	75.77	76.50
		1.25	4	75.83	0.76	75.18	76.91
		1.5	4	74.88	0.07	74.80	74.97
		1.75	4	73.83	0.95	72.77	74.85
		2	4	72.75	1.16	71.21	73.74
	Rec	1	4	79.54	0.53	79.05	80.21
		1.25	4	76.32	0.09	76.23	76.44
		1.5	4	74.25	0.40	73.89	74.77
		1.75	4	72.22	0.21	72.01	72.43
		2	4	70.80	0.13	70.62	70.92

TABLE XIII  
ANOVA results for CIEL\* measured from SCI

<b>Effect</b>	<b>NumDF</b>	<b>DenDF</b>	<b>FValue</b>	<b>ProbF</b>	<b>sig</b>
Translucency	1	90	962.96	<.0001	*
Firing_Temp	2	90	306.25	<.0001	*
Thickness	4	90	140.78	<.0001	*
Transluce*Firing_Tem	2	90	295.81	<.0001	*
Translucen*Thickness	4	90	1.38	0.2472	
Firing_Tem*Thickness	8	90	41.54	<.0001	*
Transl*Firing*Thickn	8	90	3.37	0.0020	*

TABLE XIV  
The mean, standard deviation, standard error, minimum and maximum for CIEa\*  
measured from SCI

Analysis Variable: SCI a*							
Translucency	Firing Temp.	Thickness	N	Mean	SD	Minimum	Maximum
HT	750	1	4	6.53	0.09	6.40	6.61
		1.25	4	6.45	0.43	6.03	6.88
		1.5	4	5.98	0.21	5.70	6.15
		1.75	4	5.68	0.09	5.57	5.76
		2	4	5.45	0.15	5.35	5.67
	820	1	4	4.92	0.43	4.55	5.52
		1.25	4	4.40	0.38	3.88	4.75
		1.5	4	4.46	0.54	3.98	5.22
		1.75	4	3.92	0.27	3.62	4.17
		2	4	3.85	0.15	3.71	4.01
	Rec	1	4	0.99	0.06	0.91	1.04
		1.25	4	1.32	0.06	1.27	1.39
		1.5	4	1.59	0.02	1.57	1.61
		1.75	4	1.72	0.05	1.67	1.79
		2	4	1.87	0.03	1.85	1.92
LT	750	1	4	7.48	0.72	6.93	8.53
		1.25	4	7.27	0.48	6.95	7.96
		1.5	4	6.68	0.46	6.28	7.24
		1.75	4	6.07	0.33	5.79	6.45
		2	4	6.27	0.34	5.92	6.68
	820	1	4	7.27	0.49	6.69	7.78
		1.25	4	6.43	0.38	5.86	6.70
		1.5	4	6.05	0.06	5.96	6.10
		1.75	4	5.94	0.33	5.67	6.42
		2	4	5.77	0.12	5.64	5.90
	Rec	1	4	2.56	0.03	2.53	2.60
		1.25	4	3.07	0.07	2.98	3.12
		1.5	4	3.38	0.14	3.20	3.52
		1.75	4	3.64	0.04	3.60	3.68
		2	4	3.59	0.06	3.54	3.67

TABLE XV  
ANOVA results for CIEa\* measured from SCI

<b>Effect</b>	<b>NumDF</b>	<b>DenDF</b>	<b>FValue</b>	<b>ProbF</b>	<b>sig</b>
Translucency	1	90	736.18	<.0001	*
Firing_Temp	2	90	1908.09	<.0001	*
Thickness	4	90	11.78	<.0001	*
Transluce*Firing_Tem	2	90	47.96	<.0001	*
Translucen*Thickness	4	90	0.66	0.6245	
Firing_Tem*Thickness	8	90	25.04	<.0001	*
Transl*Firing*Thickn	8	90	1.17	0.3252	

TABLE XVI  
The mean, standard deviation, standard error, minimum and maximum for CIEb\*  
measured from SCI

Analysis Variable: SCI b*							
Translucency	Firing Temp.	Thickness	N	Mean	SD	Minimum	Maximum
HT	750	1	4	-9.24	0.25	-9.47	-8.95
		1.25	4	-10.27	1.13	-11.36	-9.06
		1.5	4	-9.94	0.68	-10.47	-9.03
		1.75	4	-9.70	0.34	-10.15	-9.36
		2	4	-9.61	0.59	-10.39	-8.97
	820	1	4	-4.01	1.39	-5.79	-2.70
		1.25	4	-3.09	1.50	-4.66	-1.10
		1.5	4	-4.81	2.02	-7.67	-3.00
		1.75	4	-4.03	1.07	-4.98	-2.82
		2	4	-4.17	0.42	-4.43	-3.55
	Rec	1	4	14.81	0.17	14.56	14.96
		1.25	4	15.65	0.04	15.59	15.69
		1.5	4	16.02	0.07	15.97	16.12
		1.75	4	15.82	0.05	15.76	15.87
		2	4	15.58	0.02	15.56	15.60
LT	750	1	4	-11.90	0.56	-12.59	-11.25
		1.25	4	-12.70	0.73	-13.72	-12.08
		1.5	4	-12.43	0.77	-13.35	-11.79
		1.75	4	-12.01	0.61	-12.82	-11.53
		2	4	-12.63	0.45	-13.14	-12.08
	820	1	4	-9.39	0.36	-9.70	-8.89
		1.25	4	-9.31	0.78	-9.97	-8.27
		1.5	4	-9.29	0.02	-9.32	-9.27
		1.75	4	-10.01	0.65	-10.91	-9.43
		2	4	-11.25	1.26	-12.58	-10.11
	Rec	1	4	19.61	0.11	19.52	19.77
		1.25	4	19.93	0.54	19.46	20.60
		1.5	4	19.24	0.39	18.89	19.75
		1.75	4	18.89	0.19	18.70	19.09
		2	4	17.75	0.11	17.65	17.91



TABLE XVII  
ANOVA results for CIEb\* measured from SCI

<b>Effect</b>	<b>NumDF</b>	<b>DenDF</b>	<b>FValue</b>	<b>ProbF</b>	<b>sig</b>
Translucency	1	90	140.02	<.0001	*
Firing_Temp	2	90	16463.4	<.0001	*
Thickness	4	90	3.79	0.0068	*
Transluce*Firing_Tem	2	90	393.50	<.0001	*
Translucen*Thickness	4	90	3.97	0.0051	*
Firing_Tem*Thickness	8	90	2.41	0.0209	*
Transl*Firing*Thickn	8	90	1.68	0.1149	

TABLE XVIII  
The mean, standard deviation, standard error, minimum and maximum for CIEL\*  
measured from SCE

Analysis Variable: SCE L*							
Translucency	Firing Temp.	Thickness	N	Mean	SD	Minimum	Maximum
HT	750	1	4	77.47	0.59	76.90	78.27
		1.25	4	75.61	1.09	74.62	76.96
		1.5	4	74.74	0.67	74.21	75.69
		1.75	4	75.26	0.47	74.82	75.75
		2	4	75.46	0.79	74.56	76.15
	820	1	4	80.69	1.02	79.39	81.65
		1.25	4	80.34	0.75	79.49	81.13
		1.5	4	79.03	1.31	77.09	79.83
		1.75	4	79.43	0.54	78.80	80.05
		2	4	79.47	0.10	79.36	79.58
	Rec	1	4	77.60	0.20	77.42	77.85
		1.25	4	74.24	0.75	73.39	74.96
		1.5	4	71.23	0.28	70.97	71.54
		1.75	4	68.41	0.13	68.28	68.59
		2	4	66.74	0.37	66.20	67.06
LT	750	1	4	70.92	1.28	69.02	71.76
		1.25	4	69.87	1.42	68.09	71.42
		1.5	4	69.78	1.16	68.26	70.89
		1.75	4	69.13	1.47	67.68	70.72
		2	4	67.06	0.87	66.43	68.32
	820	1	4	74.08	0.32	73.68	74.46
		1.25	4	73.46	0.93	72.64	74.80
		1.5	4	72.41	0.41	71.94	72.78
		1.75	4	71.13	1.02	69.94	72.20
		2	4	70.12	1.34	68.44	71.37
	Rec	1	4	77.54	0.73	76.83	78.43
		1.25	4	74.05	0.15	73.93	74.24
		1.5	4	71.70	0.59	71.21	72.57
		1.75	4	69.83	0.31	69.39	70.13
		2	4	68.17	0.43	67.79	68.74

TABLE XIX  
ANOVA results for CIEL\* measured from SCE

<b>Effect</b>	<b>NumDF</b>	<b>DenDF</b>	<b>FValue</b>	<b>ProbF</b>	<b>sig</b>
Translucency	1	90	867.00	<.0001	*
Firing_Temp	2	90	284.83	<.0001	*
Thickness	4	90	148.21	<.0001	*
Transluce*Firing_Tem	2	90	286.33	<.0001	*
Translucen*Thickness	4	90	3.48	0.0108	*
Firing_Tem*Thickness	8	90	35.29	<.0001	*
Transl*Firing*Thickn	8	90	3.78	0.0007	*

TABLE XX. The mean, standard deviation, standard error, minimum and maximum for CIEa\* measured from SCE.

Translucency	Firing Temp.	Thickness	N	Mean	SD	Minimum	Maximum
HT	750	1	4	6.72	0.08	6.63	6.80
		1.25	4	6.68	0.45	6.23	7.12
		1.5	4	6.23	0.23	5.92	6.41
		1.75	4	5.87	0.08	5.78	5.94
		2	4	5.64	0.18	5.50	5.89
	820	1	4	5.08	0.46	4.68	5.72
		1.25	4	4.53	0.39	4.01	4.92
		1.5	4	4.62	0.58	4.12	5.44
		1.75	4	4.05	0.29	3.72	4.32
		2	4	3.98	0.15	3.83	4.15
	Rec	1	4	1.00	0.05	0.94	1.05
		1.25	4	1.35	0.07	1.27	1.40
		1.5	4	1.63	0.02	1.60	1.65
		1.75	4	1.76	0.06	1.71	1.84
		2	4	1.90	0.04	1.87	1.96
LT	750	1	4	7.54	0.38	7.21	8.05
		1.25	4	7.55	0.49	7.17	8.27
		1.5	4	6.94	0.45	6.53	7.50
		1.75	4	6.37	0.33	6.06	6.74
		2	4	6.63	0.39	6.25	7.13
	820	1	4	7.45	0.40	6.96	7.78
		1.25	4	6.69	0.42	6.06	6.95
		1.5	4	6.31	0.11	6.18	6.42
		1.75	4	6.23	0.37	5.93	6.76
		2	4	6.05	0.15	5.87	6.21
	Rec	1	4	2.61	0.05	2.56	2.67
		1.25	4	3.15	0.08	3.05	3.21
		1.5	4	3.50	0.17	3.29	3.68
		1.75	4	3.75	0.05	3.69	3.80
		2	4	3.72	0.07	3.67	3.82

TABLE XXI  
ANOVA results for CIEa\* measured from SCE

<b>Effect</b>	<b>NumDF</b>	<b>DenDF</b>	<b>FValue</b>	<b>ProbF</b>	<b>sig</b>
Translucency	1	90	875.96	<.0001	*
Firing_Temp	2	90	2233.84	<.0001	*
Thickness	4	90	9.89	<.0001	*
Transluce*Firing_Tem	2	90	57.43	<.0001	*
Translucen*Thickness	4	90	0.48	0.7476	
Firing_Tem*Thickness	8	90	26.67	<.0001	*
Transl*Firing*Thickn	8	90	1.14	0.3425	

TABLE XXII  
The mean, standard deviation, standard error, minimum and maximum for CIEb\*  
measured from SCE

Translucency	Firing Temp.	Thickness	N	Mean	SD	Minimum	Maximum
HT	750	1	4	-9.49	0.24	-9.76	-9.22
		1.25	4	-10.60	1.17	-11.73	-9.33
		1.5	4	-10.25	0.73	-10.83	-9.29
		1.75	4	-9.99	0.36	-10.50	-9.64
		2	4	-9.82	0.62	-10.67	-9.19
	820	1	4	-4.04	1.40	-5.87	-2.71
		1.25	4	-3.32	1.09	-4.60	-2.01
		1.5	4	-4.80	2.03	-7.66	-2.93
		1.75	4	-4.01	1.10	-4.99	-2.80
		2	4	-4.20	0.41	-4.41	-3.58
	Rec	1	4	15.49	0.20	15.22	15.65
		1.25	4	16.56	0.38	16.04	16.92
		1.5	4	17.03	0.16	16.84	17.21
		1.75	4	16.83	0.23	16.50	17.03
		2	4	16.39	0.24	16.11	16.68
LT	750	1	4	-12.39	0.59	-13.17	-11.75
		1.25	4	-13.14	0.58	-13.92	-12.64
		1.5	4	-12.85	0.82	-13.78	-12.04
		1.75	4	-12.50	0.62	-13.26	-11.97
		2	4	-13.23	0.46	-13.75	-12.70
	820	1	4	-9.80	0.32	-10.13	-9.37
		1.25	4	-9.79	0.83	-10.38	-8.57
		1.5	4	-9.70	0.03	-9.74	-9.68
		1.75	4	-10.47	0.69	-11.44	-9.89
		2	4	-11.76	1.36	-13.18	-10.56
	Rec	1	4	20.56	0.19	20.37	20.82
		1.25	4	21.14	0.55	20.70	21.89
		1.5	4	20.58	0.64	20.01	21.33
		1.75	4	20.07	0.32	19.65	20.41
		2	4	19.06	0.16	18.85	19.19

TABLE XXIII  
ANOVA results for CIEb\* measured from SCE

<b>Effect</b>	<b>NumDF</b>	<b>DenDF</b>	<b>FValue</b>	<b>ProbF</b>	<b>sig</b>
Translucency	1	90	155.65	<.0001	*
Firing_Temp	2	90	17947.5	<.0001	*
Thickness	4	90	3.52	0.0102	*
Transluce*Firing_Tem	2	90	450.64	<.0001	*
Translucen*Thickness	4	90	4.19	0.0037	*
Firing_Tem*Thickness	8	90	2.64	0.0121	*
Transl*Firing*Thickn	8	90	1.49	0.1731	

TABLE XXIV

The mean, standard deviation, standard error, minimum and maximum for Translucency parameters measured from SCI

Translucency	Firing Temp	Thickness	N	Mean	SD	Minimum	Maximum
HT	750	1	4	3.60	0.12	3.45	3.75
		1.25	4	2.38	0.34	2.02	2.72
		1.5	4	1.44	0.20	1.22	1.66
		1.75	4	0.99	0.10	0.87	1.12
		2	4	0.59	0.06	0.54	0.68
	820	1	4	3.82	0.28	3.50	4.11
		1.25	4	2.75	0.29	2.37	3.03
		1.5	4	1.54	0.03	1.50	1.57
		1.75	4	1.14	0.20	0.97	1.40
		2	4	0.76	0.10	0.68	0.89
	Rec	1	4	22.47	0.23	22.21	22.73
		1.25	4	19.35	0.30	18.99	19.73
		1.5	4	16.87	0.29	16.46	17.11
		1.75	4	14.72	0.06	14.65	14.79
		2	4	13.05	0.09	12.95	13.14
LT	750	1	4	3.60	0.48	3.19	4.16
		1.25	4	2.74	0.35	2.40	3.20
		1.5	4	1.83	0.41	1.48	2.25
		1.75	4	1.27	0.17	1.05	1.47
		2	4	1.09	0.27	0.76	1.38
	820	1	4	4.09	0.68	3.19	4.67
		1.25	4	2.53	0.34	2.10	2.85
		1.5	4	1.76	0.17	1.53	1.94
		1.75	4	1.23	0.19	1.05	1.43
		2	4	0.97	0.07	0.87	1.02
	Rec	1	4	19.18	0.48	18.72	19.82
		1.25	4	15.94	0.56	15.23	16.60
		1.5	4	14.03	0.35	13.67	14.46
		1.75	4	11.94	0.21	11.66	12.17
		2	4	10.16	0.11	10.02	10.27



TABLE XXV  
ANOVA results for translucency parameter measured from SCI

<b>Effect</b>	<b>NumDF</b>	<b>DenDF</b>	<b>FValue</b>	<b>ProbF</b>	<b>sig</b>
Translucency	1	90	261.51	<.0001	*
Firing_Temp	2	90	28749.4	<.0001	*
Thickness	4	90	1089.68	<.0001	*
Transluce*Firing_Tem	2	90	401.83	<.0001	*
Translucen*Thickness	4	90	1.83	0.1294	
Firing_Tem*Thickness	8	90	182.51	<.0001	*
Transl*Firing*Thickn	8	90	0.86	0.5500	

TABLE XXVI  
Statistical analysis on SCI of the recommended temperature

Comparisons within Thickness				
Comparison	Diff of Means	t	P	P<0.050
HT vs. LT	3.042	30.938	<0.001	Yes
Comparisons within 1				
Comparison	Diff of Means	t	P	P<0.05
HT vs. LT	3.288	14.956	<0.001	Yes
Comparisons within 1.25				
Comparison	Diff of Means	t	P	P<0.05
HT vs. LT	3.408	15.501	<0.001	Yes
Comparisons within 1.5				
Comparison	Diff of Means	t	P	P<0.05
HT vs. LT	2.841	12.923	<0.001	Yes
Comparisons within 1.75				
Comparison	Diff of Means	t	P	P<0.05
HT vs. LT	2.781	12.647	<0.001	Yes
Comparisons within 2				
Comparison	Diff of Means	t	P	P<0.05
HT vs. LT	2.892	13.152	<0.001	Yes

Comparisons within HT				
Comparison	Diff of Means	t	P	P<0.05
1.000 vs. 2.000	9.420	42.843	<0.001	Yes
1.000 vs. 1.750	7.752	35.259	<0.001	Yes
1.250 vs. 2.000	6.294	28.626	<0.001	Yes
1.000 vs. 1.500	5.605	25.494	<0.001	Yes
1.250 vs. 1.750	4.626	21.042	<0.001	Yes
1.500 vs. 2.000	3.814	17.349	<0.001	Yes
1.000 vs. 1.250	3.126	14.217	<0.001	Yes
1.250 vs. 1.500	2.479	11.277	<0.001	Yes
1.500 vs. 1.750	2.147	9.765	<0.001	Yes
1.750 vs. 2.000	1.667	7.584	<0.001	Yes

TABLE XXVII  
 Statistical analysis on SCI of the recommended temperature (continue)

Comparisons within LT				
Comparison	Diff of Means	t	P	P<0.05
1.000 vs. 2.000	9.023	41.039	<0.001	Yes
1.000 vs. 1.750	7.245	32.950	<0.001	Yes
1.250 vs. 2.000	5.778	26.278	<0.001	Yes
1.000 vs. 1.500	5.158	23.461	<0.001	Yes
1.250 vs. 1.750	3.999	18.189	<0.001	Yes
1.500 vs. 2.000	3.865	17.578	<0.001	Yes
1.000 vs. 1.250	3.246	14.762	<0.001	Yes
1.500 vs. 1.750	2.086	9.490	<0.001	Yes
1.250 vs. 1.500	1.913	8.699	<0.001	Yes
1.750 vs. 2.000	1.778	8.089	<0.001	Yes

TABLE XXVIII  
 Summary of the coefficients of translucency parameters measured from SCI

Coefficient of Translucency Parameter ( $p$ ) SCI				
	HT		LT	
	Mean	SD	Mean	SD
750	1.79	0.14	1.32	0.07
820	1.67	0.21	1.44	0.11
RECOM	0.54	0.00	0.65	0.02

TABLE XXIX  
Summary of TP<sub>0</sub> measured from SCI

TP <sub>0</sub> SCI				
	HT		LT	
	Mean	SD	Mean	SD
750	22.05	4.20	13.61	1.29
820	20.90	5.40	15.92	2.27
RECOM	38.09	0.27	36.74	1.42

TABLE XXX  
 Statistical analysis on Coefficient of translucency parameters measured from SCI

Comparisons for factor: <b>within 750</b>					
<b>Comparison</b>	<b>Diff of Means</b>	<b>t</b>	<b>P</b>	<b>P&lt;0.05</b>	
HT vs. LT	0.467	5.725	<0.001	Yes	
Comparisons for factor: <b>within 820</b>					
<b>Comparison</b>	<b>Diff of Means</b>	<b>t</b>	<b>P</b>	<b>P&lt;0.05</b>	
HT vs. LT	0.222	2.720	0.014	Yes	
Comparisons for factor: <b>within RECOM</b>					
<b>Comparison</b>	<b>Diff of Means</b>	<b>t</b>	<b>P</b>	<b>P&lt;0.05</b>	
LT vs. HT	0.110	1.343	0.196	No	
Comparisons for factor: <b>within HT</b>					
<b>Comparison</b>	<b>Diff of Means</b>	<b>t</b>	<b>P</b>	<b>P&lt;0.05</b>	
750.000 vs. RECOM	1.243	15.247	<0.001	Yes	
820.000 vs. RECOM	1.123	13.775	<0.001	Yes	
750.000 vs. 820.000	0.120	1.472	0.158	No	
Comparisons for factor: <b>within LT</b>					
<b>Comparison</b>	<b>Diff of Means</b>	<b>t</b>	<b>P</b>	<b>P&lt;0.05</b>	
820.000 vs. RECOM	0.792	9.712	<0.001	Yes	
750.000 vs. RECOM	0.667	8.178	<0.001	Yes	
820.000 vs. 750.000	0.125	1.533	0.143	No	

TABLE XXXI

The mean, standard deviation, standard error, minimum and maximum for Translucency parameters measured from SCE

Translucency	Firing Temp	Thickness	N	Mean	SD	Minimum	Maximum
HT	750	1	4	3.70	0.12	3.55	3.82
		1.25	4	2.51	0.27	2.24	2.80
		1.5	4	1.48	0.20	1.25	1.68
		1.75	4	1.02	0.11	0.89	1.16
		2	4	0.60	0.07	0.55	0.69
	820	1	4	3.84	0.34	3.51	4.19
		1.25	4	2.63	0.31	2.33	2.97
		1.5	4	1.71	0.14	1.51	1.81
		1.75	4	1.18	0.20	1.00	1.43
		2	4	0.77	0.08	0.69	0.88
	Rec	1	4	23.20	0.36	22.68	23.45
		1.25	4	20.24	0.31	19.87	20.57
		1.5	4	17.76	0.46	17.16	18.26
		1.75	4	15.38	0.29	14.96	15.60
		2	4	13.61	0.18	13.43	13.84
LT	750	1	4	3.98	0.57	3.44	4.79
		1.25	4	2.80	0.29	2.49	3.16
		1.5	4	1.86	0.39	1.53	2.36
		1.75	4	1.30	0.29	0.95	1.64
		2	4	0.99	0.35	0.63	1.44
	820	1	4	4.19	0.68	3.30	4.81
		1.25	4	2.63	0.31	2.20	2.93
		1.5	4	1.99	0.37	1.60	2.45
		1.75	4	1.33	0.21	1.13	1.52
		2	4	1.08	0.22	0.90	1.41
	Rec	1	4	19.99	0.53	19.49	20.49
		1.25	4	16.51	0.42	15.88	16.81
		1.5	4	14.72	0.28	14.47	15.01
		1.75	4	12.45	0.19	12.22	12.65
		2	4	10.74	0.10	10.61	10.86

TABLE XXXII  
ANOVA results translucency parameters measured from SCE

<b>Effect</b>	<b>NumDF</b>	<b>DenDF</b>	<b>FValue</b>	<b>ProbF</b>	<b>sig</b>
Translucency	1	90	218.29	<.0001	*
Firing Temp.	2	90	26372.8	<.0001	*
Thickness	4	90	967.13	<.0001	*
Transluce*Firing Temp	2	90	374.81	<.0001	*
Transluce*Thickness	4	90	1.54	0.1974	
Firing Temp*Thickness	8	90	158.27	<.0001	*
Transl*Firing*Thickn	8	90	0.62	0.7591	



TABLE XXXIII  
 Statistical analysis on Translucency parameters measured from SCE for the recommended group

Comparisons within Thickness				
Comparison	Diff of Means	t	P	P<0.050
HT vs. LT	3.158	29.477	<0.001	Yes
Comparisons within 1				
Comparison	Diff of Means	t	P	P<0.05
HT vs. LT	3.213	13.416	<0.001	Yes
Comparisons within 1.25				
Comparison	Diff of Means	t	P	P<0.05
HT vs. LT	3.736	15.596	<0.001	Yes
Comparisons within 1.5				
Comparison	Diff of Means	t	P	P<0.05
HT vs. LT	3.038	12.685	<0.001	Yes
Comparisons within 1.75				
Comparison	Diff of Means	t	P	P<0.05
HT vs. LT	2.929	12.229	<0.001	Yes
Comparisons within 2				
Comparison	Diff of Means	t	P	P<0.05
HT vs. LT	2.871	11.987	<0.001	Yes

Comparisons within HT				
Comparison	Diff of Means	t	P	P<0.05
1.000 vs. 2.000	9.592	40.043	<0.001	Yes
1.000 vs. 1.750	7.823	32.658	<0.001	Yes
1.250 vs. 2.000	6.629	27.676	<0.001	Yes
1.000 vs. 1.500	5.442	22.717	<0.001	Yes
1.250 vs. 1.750	4.861	20.292	<0.001	Yes
1.500 vs. 2.000	4.150	17.325	<0.001	Yes
1.000 vs. 1.250	2.962	12.366	<0.001	Yes
1.250 vs. 1.500	2.479	10.351	<0.001	Yes
1.500 vs. 1.750	2.381	9.941	<0.001	Yes
1.750 vs. 2.000	1.769	7.385	<0.001	Yes

TABLE XXXIV  
 Statistical analysis on Translucency parameters measured from SCE for the  
 recommended group (continue)

Comparisons within LT				
Comparison	Diff of Means	t	P	P<0.05
1.000 vs. 2.000	9.249	38.614	<0.001	Yes
1.000 vs. 1.750	7.539	31.472	<0.001	Yes
1.250 vs. 2.000	5.765	24.067	<0.001	Yes
1.000 vs. 1.500	5.267	21.986	<0.001	Yes
1.250 vs. 1.750	4.054	16.925	<0.001	Yes
1.500 vs. 2.000	3.983	16.628	<0.001	Yes
1.000 vs. 1.250	3.485	14.547	<0.001	Yes
1.500 vs. 1.750	2.272	9.485	<0.001	Yes
1.250 vs. 1.500	1.782	7.439	<0.001	Yes
	1.750 vs. 2.000	1.711	7.142	<0.001 Yes

TABLE XXXV  
Summary of the coefficient of translucency parameter measured from SCE

Coefficient of Translucency Parameter ( $p$ ) SCE				
	HT		LT	
	Mean	SD	Mean	SD
750	1.81	0.15	1.50	0.31
820	1.62	0.20	1.37	0.14
RECOM	0.54	0.01	0.64	0.03

TABLE XXXVI  
Summary for TP<sub>0</sub> measured from SCE

TP <sub>0</sub> SCE				
	HT		LT	
	Mean	SD	Mean	SD
750	23.70	4.68	19.33	9.83
820	20.01	5.74	15.47	3.10
RECOM	39.35	0.70	37.58	1.46

TABLE XXXVII  
Statistical analysis on coefficient of translucency parameter measured from SCE

Comparisons for factor: <b>within 750</b>				
<b>Comparison</b>	<b>Diff of Means</b>	<b>t</b>	<b>P</b>	<b>P&lt;0.05</b>
HT vs. LT	0.315	2.570	0.019	Yes
Comparisons for factor: <b>within 820</b>				
<b>Comparison</b>	<b>Diff of Means</b>	<b>t</b>	<b>P</b>	<b>P&lt;0.05</b>
HT vs. LT	0.252	2.055	0.055	No
Comparisons for factor: <b>within RECOM</b>				
<b>Comparison</b>	<b>Diff of Means</b>	<b>t</b>	<b>P</b>	<b>P&lt;0.05</b>
LT vs. HT	0.102	0.829	0.418	No
Comparisons for factor: <b>within HT</b>				
<b>Comparison</b>	<b>Diff of Means</b>	<b>t</b>	<b>P</b>	<b>P&lt;0.05</b>
750.000 vs. RECOM	1.277	10.426	<0.001	Yes
820.000 vs. RECOM	1.088	8.887	<0.001	Yes
750.000 vs. 820.000	0.189	1.539	0.141	No
Comparisons for factor: <b>within LT</b>				
<b>Comparison</b>	<b>Diff of Means</b>	<b>t</b>	<b>P</b>	<b>P&lt;0.05</b>
750.000 vs. RECOM	0.861	7.027	<0.001	Yes
820.000 vs. RECOM	0.735	6.003	<0.001	Yes
750.000 vs. 820.000	0.125	1.025	0.319	No

SUMMARY AND CONCLUSION

In this project, we developed a modified Beer-Lambert law to describe the parameters governing the effect of thickness on the light transmission in dental ceramic materials. We also applied the same equation to describe the translucency parameter. The parameters defined in these equations allow us to compare the optical properties of dental ceramic material independent of the thickness of the samples.

Furthermore, the translucency parameter of the LT IPS e.max® CAD material decreases at higher rate than the HT IPS e.max® CAD material when the thickness increases. Dentists should be aware of the fact that by increasing the thickness of IPS e.max® CAD materials, the LT IPS e.max® CAD material become more opaque faster than the HT IPS e.max® CAD.

Finally, the coefficient of absorption of LT IPS e.max® CAD is higher than the HT IPS e.max® CAD. Dentists should be aware of the fact that by increasing the thickness of IPS e.max® CAD materials, the amount of time that required to reach the same level energy increases faster for the LT IPS e.max® CAD.

REFERENCES



1. Kelly JR, Benetti P. Ceramic materials in dentistry: historical evolution and current practice. *Australian Dental Journal* 2011;56(S1):84-96.
2. McLean JW. Evolution of dental ceramics in the twentieth century. *The Journal of Prosthetic Dentistry* 2001;85(1):61-66.
3. Heffernan MJ, Aquilino SA, Diaz-Arnold AM, et al. Relative translucency of six all-ceramic systems. Part II: Core and veneer materials. *The Journal of Prosthetic Dentistry* 2002;88(1):10-15.
4. Conrad HJ, Seong W-J, Pesun IJ. Current ceramic materials and systems with clinical recommendations: A systematic review. *The Journal of Prosthetic Dentistry* 2007;98(5):389-404.
5. Rizkalla A, Jones D. Mechanical properties of commercial high strength ceramic core materials. *Dental materials* 2004;20(2):207-12.
6. Goodacre CJ, Bernal G, Rungcharassaeng K, Kan JY. Clinical complications in fixed prosthodontics. *J Prosthet Dent* 2003;90(1):31-41.
7. Lien W, Roberts HW, Platt JA, et al. Microstructural evolution and physical behavior of a lithium disilicate glass-ceramic. *Dental Materials* 2015;31(8):928-40.
8. Sakaguchi RL, Powers JM. *Craig's restorative dental materials: Elsevier Health Sciences*; 2012, 253-275.
9. Griggs JA. Recent Advances in Materials for All-Ceramic Restorations. *Dental clinics of North America* 2007;51(3):713-27.
10. Kelly JR. Dental Ceramics: what is this stuff anyway? *The Journal of the American Dental Association* 2008;139(S4):S4-S7.
11. Scientific Documentation IPS e.max® CAD. In: Ivoclar Vivadent AG RD, editor. FL-9494 Schaan, Liechtenstein; 2005.
12. Li RWK, Chow TW, Matinlinna JP. Ceramic dental biomaterials and CAD/CAM technology: State of the art. *Journal of prosthodontic research* 2014;58(4):208-16.
13. Anusavice KJ, Phillips RW. *Phillips' science of dental materials: Saunders*; 2003.
14. Giordano R, McLaren EA. Ceramics overview: classification by microstructure and processing methods. *Compendium of continuing education in dentistry* 2010;31(9):682-4.
15. McLaren EA, Terry DA. CAD/CAM systems, materials, and clinical guidelines for all-ceramic crowns and fixed partial dentures. *Compendium of continuing education in dentistry* 2002;23(7):637-41.
16. Reiss B, Walther W. Clinical long-term results and 10-year Kaplan-Meier analysis of Cerec restorations. *International Journal of Computerized Dentistry* 2000;3(1):9-23.
17. Denry I, Kelly JR. Emerging Ceramic-based Materials for Dentistry. *Journal of Dental Research* 2014;93(12):1235-42.
18. Shenoy A, Shenoy N. Dental ceramics: An update. *Journal of conservative dentistry* 2010;13(4):195-203.
19. Saint-Jean SJ. Dental Glasses and Glass-ceramics. *Advanced Ceramics for Dentistry* 2013:255-277
20. Holand W, Beall GH. *Glass ceramic technology: John Wiley & Sons*; 2012.

21. Van Noort R, Barbour ME. Introduction to Dental Materials: Elsevier Health Sciences; 2013.
22. Adair P, Grossman D. The castable ceramic crown. The International journal of periodontics & restorative dentistry 1983;4(2):32-46.
23. McLaren EA, White SN. Glass-infiltrated zirconia/alumina-based ceramic for crowns and fixed partial dentures. Practical periodontics and aesthetic dentistry 1999;11(8):985-94.
24. Duret F, Blouin J-L, Duret B. CAD-CAM in dentistry. The Journal of the American Dental Association 1988;117(6):715-20.
25. McLaren EA, Figueira J. Updating Classifications of Ceramic Dental Materials: A Guide to Material Selection. Compendium of continuing education in dentistry 2015;36(6):400-5.
26. Denry I, Holloway J. Ceramics for Dental Applications: A Review. Materials 2010;3(1):351-368.
27. Denry I, Abushaban R, Holloway J. Microstructure, crack patterns and flexural strength of two machinable dental ceramics. Journal of Dental Research 1999;78:473.
28. Tinschert J, Natt G, Hassenpflug S, Spiekermann H. Status of current CAD/CAM technology in dental medicine. International journal of computerized dentistry 2004;7(1):25-45.
29. Filser F. Direct ceramic machining of dental restorations. Ph.D. Thesis; Swiss Federal Institute of Technology, Zurich, 2001.
30. Guazzato M, Albakry M, Ringer SP, Swain MV. Strength, fracture toughness and microstructure of a selection of all-ceramic materials. Part I. Pressable and alumina glass-infiltrated ceramics. Dental Materials 2004;20(5):441-48.
31. Stookey S. Catalyzed crystallization of glass in theory and practice. Industrial & Engineering Chemistry 1959;51(7):805-08.
32. Datla SR, Alla RK, Alluri VR, Babu J, Konakanchi A. Dental Ceramics: Part II—Recent Advances in Dental Ceramics. American Journal of Materials Engineering and Technology 2015;3(2):19-26.
33. Apel E, Höland W, Schweiger M, et al. Lithium silicate glass ceramic: Patent US9232989 B2; 2008.
34. Bischoff C, Eckert H, Apel E, Rheinberger VM, Höland W. Phase evolution in lithium disilicate glass–ceramics based on non-stoichiometric compositions of a multi-component system: structural studies by  $^{29}\text{Si}$  single and double resonance solid state NMR. Physical Chemistry Chemical Physics 2011;13(10):4540-51.
35. BOROM MP, TURKALO AM, Doremus RH. Strength and Microstructure in Lithium Disilicate Glass-Ceramics. Journal of the American Ceramic Society 1975;58(9-10):385-91.
36. Wen G, Zheng X, Song L. Effects of  $\text{P}_2\text{O}_5$  and sintering temperature on microstructure and mechanical properties of lithium disilicate glass-ceramics. Acta materialia 2007;55(10):3583-91.
37. Höland W, Apel E, van't Hoen C, Rheinberger V. Studies of crystal phase formations in high-strength lithium disilicate glass–ceramics. Journal of non-crystalline solids 2006;352(38):4041-50.

38. Huang S, Cao P, Li Y, Huang Z, Gao W. Nucleation and crystallization kinetics of a multicomponent lithium disilicate glass by in situ and real-time synchrotron x-ray diffraction. *Crystal Growth & Design* 2013;13(9):4031-38.
39. Huang S, Huang Z, Gao W, Cao P. In Situ High-Temperature Crystallographic Evolution of a Nonstoichiometric  $\text{Li}_2\text{O} \cdot 2\text{SiO}_2$  Glass. *Inorganic chemistry* 2013;52(24):14188-95.
40. Huang S, Huang Z, Gao W, Cao P. Structural Response of Lithium Disilicate in Glass Crystallization. *Crystal Growth & Design* 2014;14(10):5144-51.
41. Apel E, van't Hoen C, Rheinberger V, Höland W. Influence of  $\text{ZrO}_2$  on the crystallization and properties of lithium disilicate glass-ceramics derived from a multi-component system. *Journal of the European Ceramic Society* 2007;27(2):1571-77.
42. O'Brien WJ. *Dental materials and their selection*: Quintessence; 2002.
43. Paravina RD. *Esthetic color training in dentistry*: Mosby; 2004.
44. Chu SJ DA, Paravina R, Mieleszko A. *Fundamentals of color: shade matching and communication in esthetic dentistry*. Quintessence; 2010.
45. O'Brien W. Double layer effect and other optical phenomena related to esthetics. *Dental Clinics of North America* 1985;29(4):667-72.
46. Vivadent I. *IPS e. max lithium disilicate: The future of all-ceramic dentistry—material science, practical applications, keys to success*. Amherst, NY: Ivoclar Vivadent 2009:1-15.
47. Della Bona A, Nogueira AD, Pecho OE. Optical properties of CAD–CAM ceramic systems. *Journal of Dentistry* 2014;42(9):1202-09.
48. O'Keefe KL, Pease PL, Herrin HK. Variables affecting the spectral transmittance of light through porcelain veneer samples. *The Journal of Prosthetic Dentistry* 1991;66(4):434-38.
49. Pick B, Gonzaga CC, Junior WS, et al. Influence of curing light attenuation caused by aesthetic indirect restorative materials on resin cement polymerization. *Eur J Dent* 2010;4(3):314-23.
50. Antonson SA, Anusavice KJ. Contrast ratio of veneering and core ceramics as a function of thickness. *International Journal of Prosthodontics* 2001;14(4):316-320.
51. Wang F, Takahashi H, Iwasaki N. Translucency of dental ceramics with different thicknesses. *The Journal of Prosthetic Dentistry* 2013;110(1):14-20.
52. Kingery W, Bowen H. K.; Uhlmann, DR. *Introduction to Ceramics*: Wiley & Sons; 1976.
53. Lee Y-K. Influence of filler on the difference between the transmitted and reflected colors of experimental resin composites. *Dental Materials* 2008;24(9):1243-47.
54. Johnston WM, Ma T, Kienle BH. Translucency parameter of colorants for maxillofacial prostheses. *The International journal of prosthodontics* 1994;8(1):79-86.
55. Barizon KT, Bergeron C, Vargas MA, et al. Ceramic materials for porcelain veneers: part II. Effect of material, shade, and thickness on translucency. *The Journal of prosthetic dentistry* 2014;112(4):864-70.

56. Barizon KTL, Bergeron C, Vargas MA, et al. Ceramic materials for porcelain veneers. Part I: Correlation between translucency parameters and contrast ratio. *The Journal of Prosthetic Dentistry* 2013;110(5):397-401.
57. Powers JM, Dennison JB, Lepeak PJ. Parameters that affect the color of direct restorative resins. *Journal of Dental Research* 1978;57(9):876-80.
58. Barizon KT, Bergeron C, Vargas MA, et al. Ceramic materials for porcelain veneers. Part I: Correlation between translucency parameters and contrast ratio. *The Journal of prosthetic dentistry* 2013;110(5):397-401.
59. Spink LS, Rungruanant P, Megremis S, Kelly JR. Comparison of an absolute and surrogate measure of relative translucency in dental ceramics. *Dental Materials* 2013;29(6):702-07.
60. Vichi A, Carrabba M, Paravina R, Ferrari M. Translucency of Ceramic Materials for CEREC CAD/CAM System. *Journal of Esthetic and Restorative Dentistry* 2014;26(4):224-31.
61. Awad D, Stawarczyk B, Liebermann A, Ilie N. Translucency of esthetic dental restorative CAD/CAM materials and composite resins with respect to thickness and surface roughness. *The Journal of Prosthetic Dentistry* 2015;113(6):534-40.
62. Harada K, Raigrodski AJ, Chung K-H, et al. A comparative evaluation of the translucency of zirconias and lithium disilicate for monolithic restorations. *The Journal of prosthetic dentistry* 2016, in press.
63. Ozturk O, Uludag B, Usumez A, Sahin V, Celik G. The effect of ceramic thickness and number of firings on the color of two all-ceramic systems. *The Journal of prosthetic dentistry* 2008;100(2):99-106.
64. Brainard DH. Color appearance and color difference specification. *The science of color* 2003;2:191-216.
65. Schanda J. *Colorimetry: understanding the CIE system*: John Wiley & Sons; 2007.
66. De Souza G, Braga RR, Cesar PF, Lopes GC. Correlation between clinical performance and degree of conversion of resin cements: a literature review. *Journal of Applied Oral Science* 2015;23(4):358-68.
67. De Azevedo Cubas GB, Camacho GB, Demarco FF, Pereira-Cenci T. The Effect of Luting Agents and Ceramic Thickness on the Color Variation of Different Ceramics against a Chromatic Background. *European Journal of Dentistry* 2011;5(3):245-52.
68. Johnston WM. Color measurement in dentistry. *Journal of Dentistry* 2009;37, (S1):e2-e6.
69. Lim H-N, Yu B, Lee Y-K. Spectroradiometric and spectrophotometric translucency of ceramic materials. *The Journal of Prosthetic Dentistry* 2010;104(4):239-46.
70. Chu SJ, Trushkowsky RD, Paravina RD. Dental color matching instruments and systems. Review of clinical and research aspects. *Journal of dentistry* 2010;38(S2):e2-e16.
71. Kim-Pusateri S, Brewer JD, Davis EL, Wee AG. Reliability and accuracy of four dental shade-matching devices. *The Journal of prosthetic dentistry* 2009;101(3):193-99.
72. Kelly JR, Nishimura I, Campbell SD. Ceramics in dentistry: Historical roots and current perspectives. *The Journal of Prosthetic Dentistry* 1996;75(1):18-32.

73. Luo XP, Zhang L. Effect of Veneering Techniques on Color and Translucency of Y-TZP. *Journal of Prosthodontics* 2010;19(6):465-70.
74. Bachhav VC, Aras MA. The effect of ceramic thickness and number of firings on the color of a zirconium oxide based all ceramic system fabricated using CAD/CAM technology. *The Journal of Advanced Prosthodontics* 2011;3(2):57-62.
75. Komori P, Paula A, Martin A, et al. Effect of light energy density on conversion degree and hardness of dual-cured resin cement. *Operative dentistry* 2010;35(1):120-24.
76. Pereira C, Magalhães C, Daleprane B, et al. LED and Halogen Light Transmission through a CAD/CAM Lithium Disilicate Glass-Ceramic. *Brazilian Dental Journal* 2015;26(6):648-53.
77. Watts D, Cash A. Analysis of optical transmission by 400–500 nm visible light into aesthetic dental biomaterials. *Journal of Dentistry* 1994;22(2):112-17.

ABSTRACT

OPTICAL PROPERTIES OF CAD-CAM LITHIUM DISILICATE  
GLASS-CERAMIC IN DIFFERENT FIRING  
TEMPERATURES AND THICKNESSES

by

Nasser Alqahtani

Indiana University School of Dentistry

Indianapolis, Indiana

Background: With the emerging of digital dentistry, IPS e.max® CAD lithium disilicate (LD) glass-ceramic material has become one of the most popular esthetic restorative materials in digital assisted dental esthetic restoration. The mechanical and optical properties of this material have been investigated in several studies. However, there is a lack of information and consensus regarding the optical properties of IPS e.max® LD glass-ceramic materials.

Objectives: 1) To investigate the optical properties as translucency parameters (TP), Contrast ratio (CR), light transmissions (Lt) and color changes (CC) between high-translucent (HT) and low-translucent (LT) IPS e.max® CAD LD glass-ceramic materials with different crystalline phases and thickness in different firing stages. 2) To investigate the optical properties as TP, CR, Lt and CC of each translucent (HT and LT) IPS e.max® CAD LD glass-ceramic materials with different crystalline phases and thickness in different firing stages. 3) To determine the mathematical relationships of thicknesses of IPS e.max® CAD LD glass-ceramics materials with TP and Lt. Materials and methods: The total of 120 of shade A2 IPS max CAD samples (HT and LT) were prepared into

square shape (15.25 mm X 15.25 mm) and were divided into two main groups according to the material translucency (HT and LT) (n=60). Each main group was further divided into 5 sub-groups according to the thickness (1.00, 1.25, 1.5, 1.75, and 2.00 mm) (n=12). Each thickness group was assigned into three groups based on different crystallization (firing) temperatures (750, 820 °C in single stage heating schedule with 1 second and 10 second holding times, respectively, and 840 °C with two-stage heating schedule (RECOM) (820°C, 840 °C with 10 second and 7 min holding time, respectively) as recommended by manufacturer (n=4). CIEL\*a\*b\*, TP, CR, and Lt were measured and calculated for all samples.

Statistical analysis: The effects of the test results were evaluated using 3-way ANOVA with factors for Translucency (HT and LT), Firing Temperature (750, 850, and RECOM) and Thickness (1, 1.25, 1.5, 1.75, and 2), as well as all two-way and three-way interactions among the factors. Pair-wise comparisons were made using Least Significant Differences to control the overall significance level at 5%.

Results: The mean irradiance and TP for both HT and LT decrease as the thickness of the samples increases from 1 to 2mm with significant difference between the thickness groups within each material translucency groups (HT and LT) and between both HT and LT. The coefficients of absorption (c) of the two materials were calculated. The effective incidence irradiance when material thickness approaches zero ( $I_e$ ) was also calculated. There is an unexpected spectral peak shift as the thickness of the samples increases. There is no statistically significant difference in  $I_e$  at 750°C and 820 °C between the HT and LT. However, there is a statistically significant higher  $I_e$  in HT at the recommended firing temperature as expected. Coefficients of translucency parameter (p)



of the materials in various firing temperature were defined and the TP of the material as the thickness approaches zero were calculated ( $TP_0$ ). The TP of the materials is directly correlated to the mean irradiance passing through the samples. There is no statistically significant difference in the  $TP_0$  and  $I_e$  of the HT and LT groups at the recommended firing temperature.

Conclusion: In this project we developed modified Beer-Lambert law to describe the parameters governing the effect of thickness on light transmission in dental ceramic material. We also applied the same equation to describe the translucency parameter. The parameters defined in these equations allow us to compare the optical property of dental ceramic material independent of the thickness of the samples.

## CURRICULUM VITAE

## Nasser M Alqahtani

Nov 11, 1985	Born in Khamais Mushait, Saudi Arabia
Jun 2003- Jul 2009	BDS, King Khalid University College of Dentistry, Abha, Saudi Arabia.
Aug 2010- Jul 2011	Internship program, King Khalid University College of Dentistry, Abha, Saudi Arabia.
Oct 2011-now	Demonstrator, King Khalid University College of Dentistry, Abha, Saudi Arabia.
Aug 2011- Dec 2011	Visiting scholar, Department of Prosthodontics, Indiana University School of Dentistry, Indiana, IN, USA.
Jun 2012- Jun 2015	Certificate in Advanced Graduate Prosthodontics, Indiana University School of Dentistry, Indiana, IN, USA.
May 2013- May 2016	Teaching assistant, Indiana University School of Dentistry, Indiana, IN, USA.
Jul 2015-Jun 2016	Maxillofacial Prosthetics Fellowship, Indiana University School of Dentistry, Indiana, IN, USA.

### Professional Organizations

The Saudi Dental Society

The International and American Association for Dental Research

The American Dental Education Association

The American Dental Association

The American College of Prosthodontists

The John F. Johnston Society

The American Academy of Maxillofacial Prosthetics

The Academy of Osseointegration

The Royal College of Dentists of Canada

The International Team for Implantology